Inorganic Chemistry
Article

Inorg. Chem. **2010**, *49*, 5143–5156 **5143**
DOI: 10.1021/ic100232s

NCN Trianionic Pincer Ligand Precursors: Synthesis of Bimetallic, Chelating Diamide, and Pincer Group IV Complexes

Soumya Sarkar, Kevin P. McGowan, Jeffrey A. Culver, Adam R. Carlson, Jürgen Koller, Andrew J. Peloquin, Melanie K. Veige, Khalil A. Abboud, and Adam S. Veige*

Center for Catalysis, University of Florida, P.O. Box 117200, Gainesville, Florida 32611

Received February 9, 2010

This report details the synthesis of new NCN trianionic pincer ligand precursors and metalation reactions to form group (IV) complexes. *N*,*N*′-[1,3-phenylenebis(methylene)]bis-2,6-diisopropylaniline [2,6-^{i}PrNCN]H$_3$ (**8**) was converted to the *N*,*N*′-substituted Si(IV), Sn(IV), Mg(II), and Zn(II) derivatives. [2,6-^{i}PrNCHN](SiMe$_3$)$_2$ (**9-Si**) and [2,6-^{i}PrNCHN](SnMe$_3$)$_2$ (**9-Sn**) form by first treating **8** with MeLi followed by Me$_3$MCl, where M = Si or Sn. Single crystal X-ray experiments indicate **8**, **9-Si**, and **9-Sn** have similar structural features in the solid state. [2,6-^{i}PrNCHN](μ-MgCl·THF)$_2$ (**12**) forms by treating **8** with MeMgCl, and its solid state structure revealed a *bis*-μ-MgCl bridging unit. The ^{1}H NMR spectrum of **12** reveals a dynamic process occurs in solution. A variable temperature ^{1}H NMR experiment failed to quench the dynamic process. {[2,6-^{i}PrNCHN]Zn}$_2$ (**13**) forms upon treating {[2,6-^{i}PrNCHN]Li$_2$}$_2$ (**10**) with anhydrous ZnCl$_2$ and is a dimer in the solid state. Again, dynamic ^{1}H NMR behavior is observed, and a mechanism is provided to explain the apparent low symmetry of **13** in solution. Extension of the aliphatic arm of the NCN ligand provides the new N^{C}C^{C}N pincer ligand precursors *N*,*N*′-(2,2′-(1,3-phenylene)bis(ethane-2,1-diyl))bis(3,5-bis(trifluoromethyl)aniline) [3,5-CF$_3$N^{C}C^{C}N]H$_3$ (**16**) and [3,5-CF$_3$N^{C}CH^{C}N](SiMe$_3$)$_2$ (**17**). A more rigid ligand architecture was accessed by synthesis of the anthracene derived pincer ligand anthracene-1,8-diylbis(*N*-3,5-bistrifluormethylaniline) [3,5-CF$_3$N^{C}C$_{anth}$^{C}N]H$_3$ (**18**). Treating {Zr(NMe$_2$)$_4$}$_2$ with 2 equiv of **16** provides the dimer {(μ-3,5-CF$_3$N^{C}CH^{C}N)Zr(NMe$_2$)$_3$NHMe$_2$}$_2$ (**19**). Treating Hf(NMe$_2$)$_4$ with **18** provides the bimetallic complex (μ-3,5-CF$_3$N^{C}CH$_{anth}$^{C}N){Hf(NMe$_2$)$_3$NHMe$_2$}$_2$ (**20**) in which one ligand bridges two Hf(IV) ions. Salt metathesis between **10** and ZrCl$_2$(NMe$_2$)$_2$(THF)$_2$ provides the mononuclear complex [2,6-^{i}PrNCHN]Zr(NMe$_2$)$_2$ (**21**) in which the NCN ligand is bound as a chelating diamide. Thermoysis of **21** does not lead to formation of a trianionic pincer complex. Instead, treating HfCl$_4$ with {[2,6-^{i}PrNCN]Li$_3$}$_2$ (**11**) followed by MeLi provides the trianionic pincerate complex [2,6-^{i}PrNCNHfMe$_2$][Li(DME)$_2$] (**23**). In the solid state the Hf ion has distorted trigonal bipyramidal geometry.

1. Introduction

Trianionic pincers are a new and potentially general class of ligand capable of supporting reactive metal species. Figure 1 depicts seven trianionic pincer(type) ligand architectures. They constrain three anionic metal−ligand bonds to the meridional plane and, though they occupy three coordination sites, they can only contribute a maximum of 10−12 electrons (formal oxidation state method). Consequently, a broad scope of coordinatively and electronically unsaturated metal species is plausible. However, choice of ligand precursor and metal substrate determine whether effective complexes form. For example, during metalation of HfCl$_4$(THF)$_2$ with 2,6-^{i}PrNCN^{3-} (**A**), an additional Cl$^-$ ligand adds to form the pincerate complex [(2,6-^{i}PrNCN)HfCl$_2$][Li(DME)$_3$] (**1**), and the yield is low.[1] Altering the N-aryl substituent to 3,5-Me$_2$C$_6$H$_3$ results in the coordinately saturated complex [(3,5-MeNCN)$_2$Hf][Li(DME)]$_2$ (**2**), in which two ligands bind one metal.[1]

A more promising metalation approach begins with neutral pincer precursors and MR$_x$ and M(NR$_2$)$_x$ as substrates to eliminate alkane and amine, respectively. Remarkably, when metalating 3,3″,5,5″-tetra-*tert*-butyl-1,1′:3′,1″-terphenyl-2,2″-diol (**B**; R,R′ = ^{t}Bu) with Me$_3$TaCl$_2$, C−H σ-bond metathesis occurs prior to the second Ta-Me alcoholysis. This is a unique instance of high-valent metal σ-bond metathesis within the same coordination sphere as a protic group.[2] Zirconium and titanium complexes bearing dianionic bisphenolate versions of **B** with furan, thiophenes, and pyridine central rings in place of benzene are precatalysts for propylene polymerization and oligomerization.[3] Generation of a

*To whom correspondence should be addressed. E-mail: veige@chem.ufl.edu.

(1) Koller, J.; Sarkar, S.; Abboud, K. A.; Veige, A. S. *Organometallics* **2007**, *26*, 5438–5441.

(2) (a) Agapie, T.; Bercaw, J. E. *Organometallics* **2007**, *26*, 2957–2959. (b) Agapie, T.; Day, M. W.; Bercaw, J. E. *Organometallics* **2008**, *27*, 6123–6142.

(3) (a) Agapie, T.; Henling, L. M.; DiPasquale, A. G.; Rheingold, A. L.; Bercaw, J. E. *Organometallics* **2008**, *27*, 6245–6256. (b) Golisz, S. R.; Bercaw, J. E. *Macromolecules* **2009**, *42*, 8751–8762.

Published on Web 04/29/2010

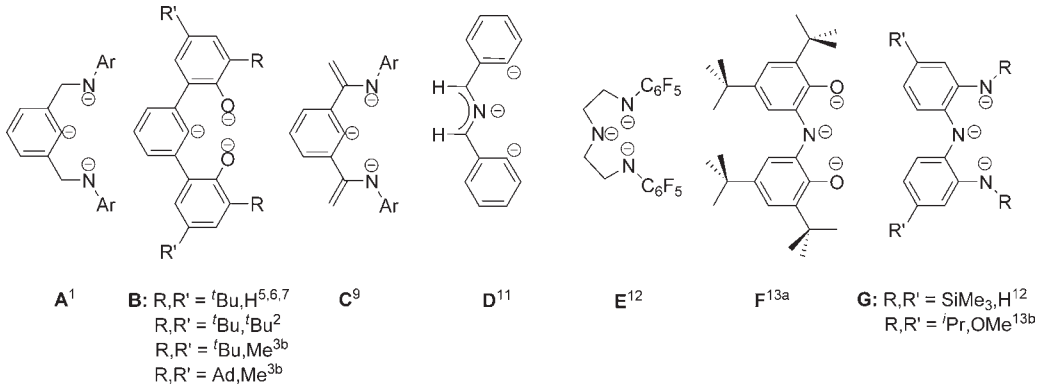

Figure 1. Seven examples of trianionic pincer(type) ligand architectures.

single component catalyst is possible when the central ring is benzene,[3b] but the activity is modest.[4]

NH bonds are also stable in the presence of pincer high-valent M−C bonds. Smooth aminolysis of $Mo(NMe_2)_4$ with the 3,3″-di-*tert*-butyl-1,1′:3′,1″-terphenyl-2,2″-diol (**B**: R,R′ = ^{t}Bu,H) results in formation of the amido-amine complex [^{t}BuOCO]MoNMe$_2$(NHMe$_2$)$_2$ (**3**).[5] Subsequent treatment of **3** with NaN_3 results in the formation of the anionic Mo-nitride dimer {[^{t}BuOCO]Mo≡N(NMe$_2$)Na(DMF)}$_2$ (**4**). Exemplifying the potential reactivity of these pincer complexes, **4** swiftly transfers its N-atom to acid chlorides (RCOCl, R = Me, Ph, ^{t}Bu) to form nitriles.[6,7] Another metalation approach involves double salt metathesis and aryl CH σ-bond metathesis. For example, the dipotassium salt of **B** (R,R′ = ^{t}Bu,H), [^{t}BuOCHO]K$_2$(THF) (**5**), reacts with MeCrCl$_2$(THF)$_3$ to from [^{t}BuOCO]Cr(THF)$_3$ (**6**), KCl, and CH_4. [^{t}BuOCO]Cr(THF)$_3$ (**6**) is an active precatalyst for the aerobic oxidation of PPh_3.[8]

In search for low-valent uranium species, Gambarotta et al. used the 1,3-[2,5-^{i}Pr$_2$PhNC(=CH)$_2$]$_2$C$_6$H$_4^{2-}$ (**7**) dianionic ligand[9] precursor to form U^{III}, and U^{IV} complexes.[10] For both U^{III} and U^{IV}, the aryl-CH bond of the central ring remains intact, and the ligands are dienamides. Somewhat unexpectedly, upon reduction, the aryl-CH bond activates creating the trianionic pincer form of the ligand (**C**), concomitant with solvent degradation. NaH or Li/naphthalene reduction leads to formation of formally U^{I} and U^{II} complexes, respectively, though DFT studies indicate extensive π-back-donation, indicating the oxidation states are more likely U^{III} and U^{IV}.[10]

Wolczanski et al. exploit 1,3-di-2-pyridyl-2-azaallyl (smif)[11] ligands to modulate the field strength of coordination compounds of the first row. Among the possible derivatives, and with the best chance to generate a very strong field complex, is the trianionic diarylazaallyl (**D**).[12] However, isolation of stable complexes bearing this form of the ligand remain elusive. Evidence supports the intermediacy of an Fe(III) complex, but H-atom abstraction occurs and the ligand converts to the dianionic imine form. Reminiscent of this, metalation reactions between the trilithio salt of **A** and MCl_x substrates often result in brightly colored solutions at −35 °C, but upon warming form intractable mixtures with stoichiometric formation of the neutral free ligand, a result of H-atom abstraction. Trianionic ONO and NNN pincer-type ligands (**E**−**G**) may be advantageous because they do not require formation of a metal−carbon bond, hence metalation is easier.[13] Recent examples indicate these ligands are non-innocent and are redox active.[14]

Metalating a multianionic ligand is challenging. To generalize this ligand-type, multiple trianionic pincer ligand precursors are necessary to accommodate the diversity of properties across the transition metal series. No trianionic pincer ligand complexes exist beyond group 6. Within this report we describe a new set of pincer ligand precursors. It is anticipated these precursors will be useful for creating new reactive fragments bearing a trianionic pincer ligand. In addition, using zirconium and hafnium as the metal substrate, herein are examples of metalations that result in bimetallic species, a mononuclear complex with an unactivated ligand C−H aryl bond, and a trianionic pincer complex. The bimetallic species are a consequence of metalating without prior activation of the aryl C−H bond of the pincer.

2. Experimental Section

General Considerations. Unless specified otherwise, all manipulations were performed under an inert atmosphere using standard Schlenk or glovebox techniques. Pentane, hexanes, toluene, diethyl ether, tetrahydrofuran (THF), and 1,2-dimethoxyethane were dried using a GlassContour drying column.

(4) [^{t}BuOCHO]Zr(CH$_2$Ph)$_2$ is a single component catalysts for ethylene polymerization (80 psi ethylene), 30 mg (0.053 mmol) [^{t}BuOCHO]Zr(CH$_2$Ph)$_2$, toluene (25 mL), triisobutylaluminum (10 equiv water scavenger), 24 h; yield 120 mg polyethylene. Kuppuswamy, S.; Veige, A. S. unpublished results.

(5) Sarkar, S.; Carlson, A. R.; Veige, M. K.; Falkowski, J. M.; Abboud, K. A.; Veige, A. S. *J. Am. Chem. Soc.* **2008**, *130*, 1116–1117.

(6) Sarkar, S.; Abboud, K. A.; Veige, A. S. *J. Am. Chem. Soc.* **2008**, *130*, 16128–16129.

(7) (a) Bindl, M.; Stade, R.; Heilmann, E. K.; Picot, A.; Goddard, R.; Furstner, A. *J. Am. Chem. Soc.* **2009**, *131*, 9468–9470. (b) Mendiratta, A.; Cummins, C. C.; Kryatova, O. P.; Rybak-Akimova, E. V.; McDonough, J. E.; Hoff, C. D. *J. Am. Chem. Soc.* **2006**, *128*, 4881–4891. (c) Figueroa, J. S.; Piro, N. A.; Clough, C. R.; Cummins, C. C. *J. Am. Chem. Soc.* **2006**, *128*, 940–950. (d) Figueroa, J. S.; Cummins, C. C. *Dalton Trans.* **2006**, 2161–2168. (e) Curley, J. J.; Sceats, E. L.; Cummins, C. C. *J. Am. Chem. Soc.* **2006**, *128*, 14036–14037. (f) Mendiratta, A.; Cummins, C. C.; Kryatova, O. P.; Rybak-Akimova, E. V.; McDonough, J. E.; Hoff, C. D. *Inorg. Chem.* **2003**, *42*, 8621–8623.

(8) O'Reilly, M.; Falkowski, J. M.; Ramachandran, V.; Pati, M.; Abboud, K. A.; Dalal, N. S.; Gray, T. G.; Veige, A. S. *Inorg. Chem.* **2009**, *48*, 10901–10903.

(9) Nuckel, S.; Burger, P. *Organometallics* **2000**, *19*, 3305–3311.

(10) Korobkov, I.; Gorelsky, S.; Gambarotta, S. *J. Am. Chem. Soc.* **2009**, *131*, 10406–10420.

(11) (a) Frazier, B. A.; Wolczanski, P. T.; Lobkovsky, E. B. *Inorg. Chem.* **2009**, *48*, 11576–11585. (b) Frazier, B. A.; Wolczanski, P. T.; Lobkovsky, E. B.; Cundari, T. R. *J. Am. Chem. Soc.* **2009**, *131*, 3428–3429.

(12) Volpe, E. C.; Wolczanski, P. T.; Lobkovsky, E. B. *Organometallics* **2010**, *29*, 364–377.

(13) Schrock, R. R.; Lee, J.; Liang, L. C.; Davis, W. M. *Inorg. Chim. Acta* **1998**, *270*, 353–362.

(14) (a) Nguyen, A. I.; Blackmore, K. J.; Carter, S. M.; Zarkesh, R. A.; Heyduk, A. F. *J. Am. Chem. Soc.* **2009**, *131*, 3307–3316. (b) Zarkesh, R. A.; Ziller, J. W.; Heyduk, A. F. *Angew. Chem., Int. Ed.* **2008**, *47*, 4715–4718.

C_6D_6 and toluene-d_8 (Cambridge Isotopes) were dried over sodium−benzophenone ketyl, distilled or vacuum transferred, and stored over molecular sieves. $CDCl_3$ (Cambridge Isotopes) was dried over anhydrous $CaCl_2$, vacuum transferred, and stored over molecular sieves. Sublimed $\{Zr(NMe_2)_4\}_2$, $Hf(NMe_2)_4$, $HfCl_4$, and $ZrCl_4$ were purchased from Strem Chemicals Co. and used without further purification. MeLi, 1.6 M in diethyl ether (Et_2O), $LiAlH_4$ (95%), *m*-xylenedicyanide (99%), and 2-bromomesitylene (99%) were purchased from Acros and used as received. Anhydrous $ZnCl_2$, $Pd_2(dba)_3$, 3,5-bis(trifluoromethyl)bromobenzene, MeMgCl (3.0 M in THF), 3,5-bis(trifluormethyl)aniline, sodium-*tert*-butoxide, chlorotrimethylsilane (97%), and trimethyltin chloride (97%) were purchased from Aldrich and used as received. *rac*-BINAP was purchased from Fluka and used as received. [2,6-^{i}PrNCN]H_3 (**8**),[15] {[2,6-^{i}PrNCHN]Li_2}$_2$ (**10**),[15] {[2,6-^{i}PrNCN]Li_3}$_2$ (**11**),[1] bis(bromomethylene)anthracene,[16] and $ZrCl_2(NMe_2)_4(THF)_2$[17] were prepared according to literature procedures. NMR spectra were obtained on Gemini (300 MHz), VXR (300 MHz), or Mercury (300 MHz) spectrometers. Chemical shifts are reported in δ (ppm). For ^{1}H and ^{13}C NMR spectra, the residual solvent peak was referenced as an internal reference. Variable temperature NMR experiments were performed in toluene-d_8. GC/MS spectra were recorded on an Agilent 6210 TOF−MS instrument. Combustion analyses were performed at Complete Analysis Laboratory Inc., Parsippany, New Jersey.

Synthesis of [2,6-^{i}PrNCHN](SiMe$_3$)$_2$ (9-Si). Chlorotrimethylsilane (122 mg, 1.12 mmol) in toluene (2 mL) was added dropwise to {[2,6-^{i}PrNCHN]Li_2}$_2$ (**10**) (250 g, 0.53 mmol) in toluene (6 mL) with stirring at −35 °C. As the solution warmed to ambient temperature over 30 min, the color turned from pale yellow to colorless. The solution was filtered through Celite and concentrated under reduced pressure. White needles were obtained from the concentrated solution after 48 h. The crystalline material was isolated by filtration and washed with cold pentane. Yield 180 mg (56%). ^{1}H NMR (300 MHz, C_6D_6) δ (ppm): 7.08 (t, J = 6 Hz, 1H, Ar-*H*), 7.05 (s, 1H, Ar-*H*), 7.00 (s, 2H, Ar-*H*), 6.98 (d, J = 3 Hz, 2H, Ar-*H*), 6.90 (d, J = 3 Hz, 4H, Ar-*H*), 6.05(bs, 1H, Ar-*H*), 3.99 (s, 4H, Ar−CH_2N), 3.25 (sept, J = 6 Hz, 4H, CH(CH$_3$)$_2$), 1.15 (d, J = 6 Hz, 12H, CH(CH_3)$_2$), 0.83 (d, J = 6 Hz, 12H, CH(CH_3)$_2$), 0.15 (s, 18H, -Si(CH_3)$_3$). ^{13}C{^{1}H} NMR (75.36 Hz, C_6D_6) δ (ppm): 149.2 (s, C aromatic), 142.3 (s, C aromatic), 140.1 (s, C aromatic), 132.7 (s, C aromatic), 129.3 (s, C aromatic), 126.6 (s, C aromatic), 124.5 (s, C aromatic), 56.0 (s, ArCH$_2$N), 28.4 (s, CH(CH$_3$)$_2$), 25.6 (s, CH(CH$_3$)$_2$), 25.1 (s, CH(CH$_3$)$_2$), 1.2 (s, -Si(CH$_3$)$_3$). Anal. Calcd for $C_{38}H_{60}N_2Si_2$: C, 75.93; H, 10.06; N, 4.66. Found: C, 76.10; H, 10.13; N, 4.86.

Synthesis of [2,6-^{i}PrNCHN](SnMe$_3$)$_2$ (9-Sn). Trimethyltinchloride (1.06 g, 5.33 mmol) in toluene (2 mL) was added dropwise to {[2,6-^{i}PrNCHN]Li_2}$_2$ (**10**) (1.19 g, 2.54 mmol) in toluene (6 mL) with stirring at −35 °C. The reaction was warmed to room temperature and stirred for 20 h. The solution was filtered through Celite and concentrated under reduced pressure. White needles were obtained from the concentrated solution after 48 h. The product was isolated by filtration and the solid washed with cold pentane. Yield 1.34 g (67.2%). ^{1}H NMR (300 MHz, C_6D_6) δ (ppm): 7.48 (s, 1H, Ar-*H*), 7.30−7.24 (m, 2H, Ar-*H*), 7.22−7.18 (m, 2H, Ar-*H*), 7.18−7.12 (m, 5H, Ar-*H*), 4.41 (s, 4H, Ar−CH_2N), 3.79 (sept, J = 6 Hz, 4H, CH(CH$_3$)$_2$), 1.32 (d, J = 6 Hz, 12H, CH(CH_3)$_2$), 1.24 (d, J = 9 Hz, 12H, CH(CH_3)$_2$), 0.04 (t, J = 27 Hz, 18H, Sn(CH_3)$_3$). ^{13}C {^{1}H} NMR (75.36 Hz, C_6D_6) δ (ppm): 149.1 (s, C aromatic), 148.5 (s, C aromatic), 142.3 (s, C aromatic), 132.7 (s, C aromatic), 129.6 (s, C aromatic), 125.7 (s, C aromatic), 124.3 (s, C aromatic), 61.6 (s, ArCH$_2$N), 28.3 (s, CH(CH$_3$)$_2$), 25.7 (s, CH(CH$_3$)$_2$), 25.2 (s, CH(CH$_3$)$_2$), −4.7 (s, Sn(CH$_3$)$_3$). Anal. Calcd for $C_{38}H_{60}N_2Sn_2$: C, 58.34; H, 7.73; N, 3.58. Found: C, 58.49; H, 7.86; N, 3.54.

Synthesis of [2,6-^{i}PrNCHN](μ-MgCl·THF)$_2$ (12). MeMgCl (5.52 mL, 3.0 M, 16.6 mmol) in THF was added dropwise to [2,6-^{i}PrNCN]H_3 (**8**) (3.69 g, 8.08 mmol) in THF (20 mL) with stirring at −35 °C. The reaction was warmed to room temperature and stirred for 1 h, and then the solution was concentrated under reduced pressure. The product was precipitated as a white powder by dropping the concentrated yellow THF solution into cold diethyl ether (15 mL). The product was isolated by filtering the solution and washing the residue with cold pentane. Yield 3.33 g (57.4%). ^{1}H NMR (300 MHz, C_6D_6) δ (ppm): 8.19 (s, 1H, Ar-*H*), 7.64 (d, J = 6 Hz, 2H, Ar-*H*), 7.38 (t, J = 8.8 Hz, 1H, Ar-*H*), 7.19 (d, J = 3 Hz, 2H, Ar-*H*), 7.09 (t, J = 3 Hz, 4H, Ar-*H*), 4.44 (s, 4H, Ar−CH_2N, overlapping), 4.42 (sept, J = 6 Hz, 4H, CH(CH$_3$)$_2$, overlapping), 3.33 (bs, 16H, OCH_2CH$_2$), 1.48 (d, J = 6 Hz, 12H, CH(CH_3)$_2$), 1.30 (d, J = 6 Hz, 12H, CH(CH_3)$_2$), 1.12 (bs, 16H, OCH$_2$CH_2). ^{13}C{^{1}H} NMR (75.36 Hz, C_6D_6) δ (ppm): 155.4 (s, C aromatic), 148.9 (s, C aromatic), 146.1 (s, C aromatic), 130.5 (s, C aromatic), 130.0 (s, C aromatic), 128.9 (s, C aromatic), 123.9 (s, C aromatic), 122.8 (s, C aromatic), 69.5 (s, OCH$_2$CH$_2$), 63.0 (s, ArCH$_2$N), 27.8 (s, CH(CH$_3$)$_2$), 27.0 (s, OCH$_2$$CH_2$), 25.5 (s, CH($CH_3$)$_2$), 25.4 (s, CH(CH$_3$)$_2$). Anal. Calcd for $C_{40}H_{58}Cl_2Mg_2N_2O_2$: C, 66.87; H, 8.14; N, 3.90. Found: C, 66.57; H, 8.03; N, 3.85.

Synthesis of {[2,6-^{i}PrNCHN]Zn}$_2$ (13). A solution of {[2,6-^{i}PrNCHN]Li_2}$_2$ (**10**) (3.015 g, 6.434 mmol) in diethyl ether (50 mL) was added to a solution of anhydrous $ZnCl_2$ (877 mg, 6.434 mmol) in diethyl ether (15 mL) at −35 °C with stirring. The reaction was warmed to room temperature, stirred for 1 h, and a white precipitate formed. The suspension was filtered to collect the product which was dried in vacuo to remove all volatiles. The solid was redissolved in chloroform (15 mL), and the solution was filtered, reduced under vacuum, and added to pentane (50 mL) with stirring to precipitate **13** as a white powder. Yield 2.276 g (2.188 mmol, 68%). X-ray quality crystals were obtained by slow evaporation from a hot benzene solution. ^{1}H NMR (300 MHz, C_6D_6) δ (ppm): 7.62 (d, 2H, J = 9 Hz, Ar-*H*), 7.46 (t, 1H, J = 7.5 Hz, Ar-*H*), 7.28 (s, 1H, Ar-*H*), 7.20 (d, 4H, J = 1.5 Hz, Ar-*H*), 7.15 (t, 2H, J = 7.5 Hz, Ar−H), 4.23 (s, 4H, Ar−CH_2N), 3.91 (sept, J = 6 Hz, 4H, CH(CH$_3$)$_2$), 1.25 (d, J = 6 Hz, 24H, CH(CH_3)$_2$). ^{13}C{^{1}H} NMR (75.36 Hz, C_6D_6) δ (ppm): 148.0 (s, C aromatic), 147.9 (s, C aromatic), 146.4 (s, C aromatic), 131.2 (s, C aromatic), 128.9 (s, C aromatic), 125.9 (s, C aromatic), 125.3 (s, C aromatic), 124.4 (s, C aromatic), 61.4 (s, ArCH$_2$N), 28.3 (s, CH(CH$_3$)$_2$), 25.2 (s, CH(CH$_3$)$_2$). Anal. Calcd for $C_{64}H_{84}N_4Zn_2$: C, 73.90; H, 8.14; N, 5.39. Found: C, 73.65; H, 8.25; N, 5.43.

Synthesis of 2,2′-(1,3-phenylene)diethanamine (15). An alternative synthesis of **15** was performed.[18] Under argon flow diethyl ether (500 mL) was added to $LiAlH_4$ (60 g, 12.7 equiv, 1.58 mmol) under stirring, in a 1000 mL three-neck flask fitted with a reflux condenser and a 500 mL dropping funnel. To the dropping funnel was added *m*-xylene dicyanide (19.4 g, 0.124 mol) in diethyl ether (300 mL). The *m*-xylene dicyanide solution was added dropwise under static argon over a period of 2 h with vigorous stirring and then refluxed under argon for 48 h. The resulting green suspension was cooled to 0 °C and quenched by adding water (100 mL) through the dropping funnel, followed by NaOH solution (15% by wt, 100 mL). Extra diethyl ether was added periodically. An additional 30 mL of water was added to produce a free-flowing white suspension. Compound **15** was extracted from the white suspension with diethyl ether (6 ×

(15) (a) Daniele, S.; Hitchcock, P. B.; Lappert, M. F.; Nile, T. A.; Zdanski, C. M. *J. Chem. Soc., Dalton Trans.* **2002**, 3980–3984. (b) Estler, F.; Eickerling, G.; Herdtweck, E.; Anwander, R. *Organometallics* **2003**, *22*, 1212–1222.

(16) Ren, J.; Zhao, X. L.; Wang, Q. C.; Ku, C. F.; Qu, D. H.; Chang, C. P.; Tian, H. *Dyes Pigm.* **2005**, *64*, 179–186.

(17) Brenner, S.; Kempe, R.; Arndt, P. *Z. Anorg. Allg. Chem.* **1995**, *621*, 2021–2024.

(18) Ruggli, P.; Prijs, B. *Helv. Chim. Acta* **1945**, *28*, 674–690.

150 mL). The organics were combined and dried over Na_2SO_4. Yellow oil was obtained by removing all volatiles under reduced pressure, and was further purified by distillation at 170 °C @ 20 mTorr. Yield 6.0 g (0.036 mol, 39%). ^{1}H NMR (300 MHz, C_6D_6) δ(ppm): 7.15 (t, J = 7.30 Hz, 1H, Ar−H), 6.99 (s, 1H, Ar−H), 6.97 (s, 2H, Ar−H), 2.88 (t, J = 6.86 Hz, 4H, -$H_2CH_2CH_2$), 2.65 (t, J = 6.86 Hz, 4H, $NH_2CH_2CH_2Ar$), 1.01 (br s, 4H, NH_2).

Synthesis of *N,N′*-(2,2′-(1,3-phenylene)bis(ethane-2,1-diyl))-bis(3,5-bis(trifluoromethyl)aniline) [3,5-$CF_3N^CC^CN$]H_3 (16). To a 100 mL round-bottom flask charged with a stir bar and toluene (50 mL) were added **15** (1.50 g, 9.15 mmol), 3,5-bis(trifluoromethyl)bromobenzene (5.37 g, 2 equiv, 18.3 mmol), $Pd_2(dba)_3$ (0.13 g, 0.5%, 0.142 mmol), *rac*-BINAP (0.23 g, 1.5%, 0.357 mmol), and NaO^{t}Bu (2.64 g, 27.5 mmol). After refluxing for 72 h under argon the solution was filtered through Celite while hot, and all volatiles were removed in vacuo. Nonvolatile products were then taken up in hot pentane and filtered again through Celite. The final product was recrystallized two times from pentane at −20 °C. Yield 2.1 g (3.57 mmol, 39%). ^{1}H NMR (300 MHz, C_6D_6) δ(ppm): 7.22 (s, 2H, Ar-*H*), 7.11 (t, J = 7.64 Hz, 1H, Ar-*H*), 6.81 (dd, J = 7.64, 1.70 Hz, 2H, Ar-*H*), 6.72 (s, 1H, Ar−H), 6.48 (s, 4H, Ar-*H*), 3.13 (t, J = 5.52 Hz, 2H, N*H*), 2.73 (dt, J = 6.94 Hz, 4H, $NHCH_2CH_2$), 2.38 (t, J = 6.94 Hz, 4H, $NHCH_2CH_2Ar$). $^{13}C\{^1H\}$ NMR (75.36 Hz, C_6D_6, δ): 149.2 (s, Ar*C*NH), 139.8 (s, $ArCCH_2-$), 133.0 (q, J_{C-F} = 32.7 Hz, -CF_3), 129.8 (s, aromatic), 127.6 (s, aromatic), 126.5 (s, aromatic), 122.9 (s, aromatic), 112.3 (s, aromatic), 110.4 (s, aromatic), 44.6 (s, $NHCH_2CH_2Ar$), 35.5 (s, $NHCH_2CH_2Ar$). HRMS calculated (found) for $C_{26}H_{20}F_{12}N_2$ $(M+H)^+$: 589.1508 (589.1537).

Synthesis of [3,5-$CF_3N^CCH^CN$]$(SiMe_3)_2$ (17). To a solution of THF (2 mL) containing **16** (1.01 g, 1.72 mmol) and a stirbar, MeMgCl (1.3 mL 3 M, 3.25 mmol) in THF (2 mL) was added dropwise at −35 °C. The solution was stirred at ambient temperature for 3 h. Chlorotrimethylsilane (610 mg, 5.65 mmol) was added at −35 °C. The solution was kept at −35 °C for 1 h then stirred at ambient temperature for 15 h. 1,4-Dioxane (2 mL) was then added causing precipitation of $MgCl_2$. The solution was filtered, and volatiles were removed in vacuo causing crystallization of the product. Yield 931 mg (1.27 mmol, 74%). ^{1}H NMR (300 MHz, C_6D_6) δ(ppm): 7.40 (s, 2H, Ar-*H*), 7.35 (s, 4H, Ar-*H*), 7.02 (t, J = 7.6 Hz, 1H, Ar-*H*), 6.77 (dd, J = 2.0, 7.61 Hz, 2H, Ar-*H*), 6.68 (s, 1H, Ar H), 3.23 (t, J = 7.5 Hz, 4H, $ArNCH_2$), 2.48 (t, J = 7.3 Hz, 4H, $ArCH_2CH_2$), 0.00 (s, 18H (15H observed), $Si(CH_3)_3$). $^{13}C\{^1H\}$ NMR (75.36 Hz, C_6D_6) δ(ppm): 150.8 (s, aromatic), 140.1 (s, aromatic), 132.8 (q, J = 32.2 Hz, CF_3), 129.9 (s, aromatic), 129.6 (s, aromatic), 129.6 (s, aromatic), 122.9 (s, aromatic), 120.8 (s, aromatic), 118.7 (s, aromatic), 112.3 (s, aromatic), 49.0 (s, CH_2NAr), 35.6 (s, -CH_2Ar), 0.7 (s, $Si(CH_3)_3$). Anal. Calcd for $C_{32}H_{36}F_{12}N_2Si_2$: C, 52.45; H, 4.95; N, 3.82. Found: C, 52.47; H, 4.82; N,3.69.

Synthesis of [3,5-$CF_3N^CC_{anth}{}^CN$]H_3 (18). To an anhydrous *N*,*N*-dimethylformamide (DMF, 15 mL) solution of bis-(bromomethylene)anthracene (2.81 g, 7.72 mmol) and K_2CO_3 was added 3,5-bis(trifluormethyl)aniline (2.65 mL, 17.0 mmol). The mixture was stirred for 15 h, and then water (50 mL) was added to form a yellow oil layer. The yellow oil was extracted with $CHCl_3$ (2 × 30 mL), washed with water, brine, dried with $MgSO_4$, and then filtered. After removing all volatiles, an oil formed with some yellow solid. The oil was dissolved in hexanes (50 mL), and the yellow solid (bis(bromomethylene)anthracene starting material) was removed by filtration. The oil contained **18**, aniline, and DMF which was separated by flash column chromatography (100 g SiO_2, 1:1 $CHCl_3$:pentane) to provide pure **18** as a pale yellow solid. Yield 2.36 g (3.57 mmol, 46%). ^{1}H NMR (300 MHz, C_6D_6, δ): 8.31 (s, 1H, Ar-*H*), 8.23 (s, 1H, Ar-*H*), 7.77 (d, J = 6 Hz, 2H, Ar-*H*), 7.40−7.00 (m, 6H, Ar-*H*), 6.49 (s, 4H, *o*-*CH*CF_3), 4.00 (d, J = 3.0 Hz, 4H, $ArNCH_2$), 3.23 (t, J = 3.0 Hz, 2H, N*H*). $^{13}C\{^1H\}$ NMR (75.36 Hz, C_6D_6) δ(ppm): 149.1 (s, *i*-*C*-NH), 133.6 (s, aromatic), 133.1 (q, J_{CF} = 33.1 Hz, CF_3), 132.7 (s, aromatic), 130.5 (s, aromatic), 129.6 (s, aromatic), 129.1 (s, aromatic), 127.0 (s, aromatic), 125.8 (s, aromatic), 119.1 (s, aromatic), 112.1 (s, aromatic), 111.0 (s, aromatic), 46.8 (s, CH_2). HRMS calculated (found) for $C_{32}H_{20}F_{12}N_2$ (M^+): 660.14 (660.1465).

Synthesis of {(μ-3,5-$CF_3N^CCH^CN$)Zr$(NMe_2)_3NHMe_2$}$_2$ (19). A solution of $\{Zr(NMe_2)_4\}_2$ (91 mg, 0.170 mmol) in toluene (1 mL) was added to **16** (200 mg, 0.340 mmol) in toluene (1 mL) at −35 °C with stirring. As the solution warmed to room temperature and stirred for 3 h, the color changed from pale yellow to brown. The solution was filtered and concentrated in vacuo. Crystallization occurred from a concentrated toluene solution of **19** over 1 week. The crystals were filtered and washed with cold pentane. Yield (222 mg, 38%). ^{1}H NMR (300 MHz, C_6D_6) δ(ppm): 7.37 (bs, 6H, Ar-*H*), 7.26 (s, 1H, Ar-*H*), 7.18 (t, J = 6 Hz, 1H, Ar-*H*), 7.11 (d, J = 6 Hz, 2H, Ar-*H*), 3.57 (m, 4H, $ArNCH_2CH_2Ar$), 2.81(s, 12H, $N(CH_3)_2$), 2.67 (m, 4H, $ArNCH_2CH_2Ar$), 1.36 (d, J = 3 Hz, 6H, $HN(CH_3)_2$), 0.90 (sept, J = 3 Hz, 2H, $HN(CH_3)_2$). $^{13}C\{^1H\}$ NMR (75.28 Hz, C_6D_6) δ(ppm): 154.9 (s, C, aromatic), 140.9 (s, C, aromatic), 133.3 (q, J = 32.3 Hz, CF_3), 130.2 (s, C, aromatic), 127.4 (s, C, aromatic), 126.8 (s, C, aromatic), 123.2 (s, C, aromatic), 115.6 (m, CF_3C), 110.3 (sept, J = 5 Hz, CF_3CCCCF_3), 50.5 (s, Zr−N$(CH_3)_2$), 42.7 (s, CCH_2CH_2), 38.8 (s, CCH_2CH_2), 35.3 (s, Zr-$NHCH_3)_2$). Anal. Calcd for $C_{64}H_{74}F_{24}N_{10}Zr_2$: C, 47.40; H, 4.60; N, 8.64. Found: C, 47.07; H, 4.66; N, 8.45.

Synthesis of (μ-3,5-$CF_3N^CCH_{anth}{}^CN$){$Hf(NMe_2)_3NHMe_2$}$_2$ (20). $Hf(NMe_2)_4$ (53.6 mg, 0.151 mmol) was added to a solution of [3,5-$CF_3N^CC_{anth}{}^CN$]H_3 (**18**) (50.0 mg, 0.076 mmol) in benzene (1 mL), and the resulting mixture was stirred for 10 min. Stirring was then stopped, and the reaction mixture was allowed to stand at room temperature for 1 h, during which a precipitate formed. The solvent was decanted, and the solid product dried in vacuo to yield **20** as a pale yellow solid (91 mg, 87%). ^{1}H NMR (300 MHz, C_6D_6) δ (ppm): 9.18 (s, 1H, Ar-*H*), 8.29 (s, 1H, Ar-*H*), 7.74 (d, J = 6 Hz, 2H, Ar-*H*), 7.63 (d, J = 6 Hz, 2H, Ar-*H*), 7.47 (s, 4H, $CCHCCF_3$), 7.30 (s, 2H, Ar-*H*, overlapping), 7.27 (dd, 2H, J = 6 Hz, J = 6 Hz, CHC*H*CH), 5.58 (s, 4H, Ar−CH_2N), 2.75 (s, 32H, Hf−$N(CH_3)_2$), 1.69 (d, J = 6 Hz, 12H, Hf-NH-$(CH_3)_2$), 0.84 (sept, J = 6 Hz, 2H, Hf−$NH(CH_3)_2$). $^{13}C\{^1H\}$ NMR (75.36 Hz, C_6D_6) δ (ppm): 158.9 (s, C aromatic), 136.2 (s, C aromatic), 132.8 (s, C aromatic), 132.2 (q, J = 31.6 Hz, CF_3), 132.1 (s, C aromatic), 130.9 (s, C aromatic), 129.8 (s, C aromatic), 128.2 (s, C aromatic), 126.0 (s, C aromatic), 124.5 (s, C aromatic), 116.6 (s, C aromatic), 115.3 (s, C aromatic), 107.8 (s, $ArCF_3$), 52.4 (s, $ArCH_2N$), 42.3 (s, Hf−$N(CH_3)_2$), 39.0 (s, Hf-$NH(CH_3)_2$). Anal. Calcd for $C_{48}H_{68}F_{12}N_{10}Hf_2$ C, 42.08; H, 5.00; N, 10.22. Found: C, 41.89; H, 4.96; N, 10.29.

Synthesis of [2,6-^{i}PrNCHN]Zr$(NMe_2)_2$ (21). $ZrCl_2(NMe_2)_4$-$(THF)_2$ (168 mg, 0.426 mmol) in Et_2O (3 mL) was added to {[2,6-^{i}PrNCHN]Li_2}$_2$ (**10**) (200 mg, 0.426 mmol) in Et_2O (3 mL) at −35 °C with stirring. As the solution was warmed to room temperature and stirred for 1 h, the color changed to pale yellow with the formation of a white precipitate. The solution was filtered, and the resulting pale yellow filtrate was concentrated in vacuo. Pentane (1 mL) was added to the solution, and the product was obtained as yellow crystals over a period of 3 days at −35 °C. Yield (114 mg, 42%). ^{1}H NMR (300 MHz, C_6D_6) δ (ppm): 9.34 (s, 1H, Ar-*H*), 7.20 (m, 4H, Ar-*H*), 7.12 (m, 3H, Ar-*H*), 6.93 (d, 2H, J = 6 Hz, Ar-*H*), 4.83 (d, 2H, J = 15 Hz, Ar−CH_2N), 4.01 (d, 2H, J = 15 Hz, Ar−CH_2N), 3.93 (sept, 2H, J = 9 Hz, $CH(CH_3)_2$), 3.70 (sept, 2H, J = 9 Hz, $CH(CH_3)_2$), 2.50 (s, 6H, $N(CH_3)_2$), 2.06 (s, 6H, $N(CH_3)_2$), 1.42 (d, 6H, J = 9 Hz, $CH(CH_3)_2$), 1.41 (d, 6H, J = 9 Hz, $CH(CH_3)_2$), 1.35 (d, 6H, J = 9 Hz, $CH(CH_3)_2$), 1.25 (d, 6H, J = 9 Hz, $CH(CH_3)_2$). $^{13}C\{^1H\}$ NMR (75.36 Hz, C_6D_6) δ(ppm): 150.3 (s, C aromatic), 146.7 (s, C aromatic), 146.3 (s, C aromatic), 145.1 (s, C aromatic), 133.7 (s, C aromatic), 127.0 (s, C aromatic), 125.4 (s, C aromatic), 124.6 (s, C aromatic), 124.2 (s, C aromatic), 63.7 (s, $ArCH_2N$), 44.0 (s, $N(CH_3)_2$), 41.4 (s, $N(CH_3)_2$), 29.3 (s, $CH(CH_3)_2$), 27.8 (s,

$CH(CH_3)_2$), 27.3 (s, $CH(CH_3)_2$), 26.9 (s, $CH(CH_3)_2$), 25.8 (s, $CH(CH_3)_2$), 25.0 (s, $CH(CH_3)_2$). Anal. Calcd for $C_{36}H_{54}N_4Zr$: C, 68.19; H, 8.58; N, 8.84. Found: C, 68.08; H, 8.64; N, 8.76.

Synthesis of [2,6-^{i}PrNCNHfMe$_2$][Li(DME)$_2$] (23). $HfCl_4$ (202 mg, 0.630 mmol) in THF (3 mL) was added to {[2,6-^{i}PrNCN]Li_3}$_2$ (**11**) (300 mg, 0.316 mmol) in THF (3 mL) at −35 °C with stirring. As the solution was warmed to room temperature and stirred for 45 min, the color changed from colorless to pale yellow. MeLi (0.78 mL, 1.6 M, 1.26 mmol) in Et_2O was added to the reaction mixture, and the stirring continued for an additional 30 min. The solution was filtered, and all volatiles were removed in vacuo. The residue was triturated and washed with pentane, and the remaining solid was extracted into DME (2 × 3 mL). The organic layers were combined, filtered, and the product was obtained as a pale yellow powder after removing the solvent in vacuo. Yield (189 mg, 35%). Single crystals for X-ray diffraction were obtained by diffusing Et_2O into a saturated DME solution of **23** at −35 °C for 4 days. ^{1}H NMR (300 MHz, $CDCl_3$) δ(ppm): 7.31−7.19 (m, 9 H, Ar-*H*), 5.21 (s, 4H, CH_2N), 4.26 (sept, 4H, J = 6 Hz, $CH(CH_3)_2$), 3.66 (s, 12H, $CH_3OCH_2CH_2O$ CH_3), 3.51 (s, 18H, $CH_3OCH_2CH_2OCH_3$), 1.41 (d, 12H, J = 3 Hz, $CH(CH_3)_2$), 1.39 (d, 12H, J = 3 Hz, $CH(CH_3)_2$), −0.49 (s, 6H, Hf-$(CH_3)_2$). $^{13}C\{^1H\}$ NMR (75.36 Hz, $CDCl_3$) δ (ppm): 205.6 (s, Hf−C aromatic), 155.6 (s, C aromatic), 154.3 (s, C aromatic), 148.4 (s, C aromatic), 124.6 (s, C aromatic), 123.0 (s, C aromatic), 122.6 (s, C aromatic), 117.4 (s, C aromatic), 72.5 (s, $ArCH_2N$), 71.0 (s, $CH_3OCH_2CH_2O$ CH_3), 59.6 (s, $CH_3OCH_2CH_2OCH_3$), 50.6 (s, Hf-CH_3), 28.8 (s, $CH(CH_3)_2$), 27.0 (s, $CH(CH_3)_2$), 24.5 (s, $CH(CH_3)_2$). Anal. Calcd for $C_{42}H_{67}HfLiN_2O_4$: C, 59.39; H, 7.95; N, 3.30. Found: C, 59.17; H, 7.92; N, 3.08.

3. Results and Discussion

Ligand Precursor Synthesis and Characterization. [2,6-^{i}PrNCHN](SiMe$_3$)$_2$ (9-Si), [2,6-^{i}PrNCHN](SnMe$_3$)$_2$ (9-Sn). Two independent reports[15] detail the synthesis of *N*, *N*′−[1,3-phenylenebis(methylene)]bis(2,6-diisopropylaniline); the parent isopropyl derivative [2,6-^{i}PrNCN]H_3 (**8**) as either a tacky oil or a crystalline solid. Free from impurities, **8** is crystalline, and large colorless crystals (2−3 cm) seed from solvent-free viscous oils of the pure substance. Figure 2A depicts the molecular structure of **8**, and Table 1 lists crystallographic data. Characterization data of **8** (^{1}H and ^{13}C NMR spectra) matches the reported values.[15]

[2,6-^{i}PrNCHN](SiMe$_3$)$_2$ (**9-Si**) and [2,6-^{i}PrNCHN](SnMe$_3$)$_2$ (**9-Sn**) form by treating {[2,6-^{i}PrNCHN]Li_2}$_2$ (**10**)[15] with Me_3SiCl and Me_3SnCl, respectively (eq 1). Compounds **9-Si** and **9-Sn** possess similar spectroscopic and solid-state properties. The ^{1}H NMR (C_6D_6) spectrum of both **9-Si** and **9-Sn** display distinct resonances for the M(CH_3)$_3$ groups, at 0.15 ppm and 0.04 ppm, respectively. The methylene protons on each derivative appear as singlets at 3.99 (**9-Si**) and 4.41 ppm (**9-Sn**), and each display two distinct isopropyl methyl resonances and a corresponding methine septet (**9-Si**, sept, 3.25 ppm, J = 6.0 Hz; **9-Sn**, sept, 3.79 ppm, J = 6 Hz).

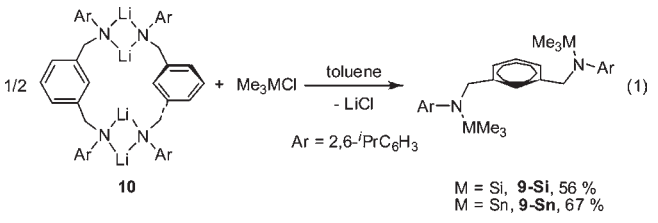

Figure 2B and 2C depict the solid-state molecular structures of **9-Si** and **9-Sn**, Table 1 lists pertinent crystallographic information, and the Supporting Information

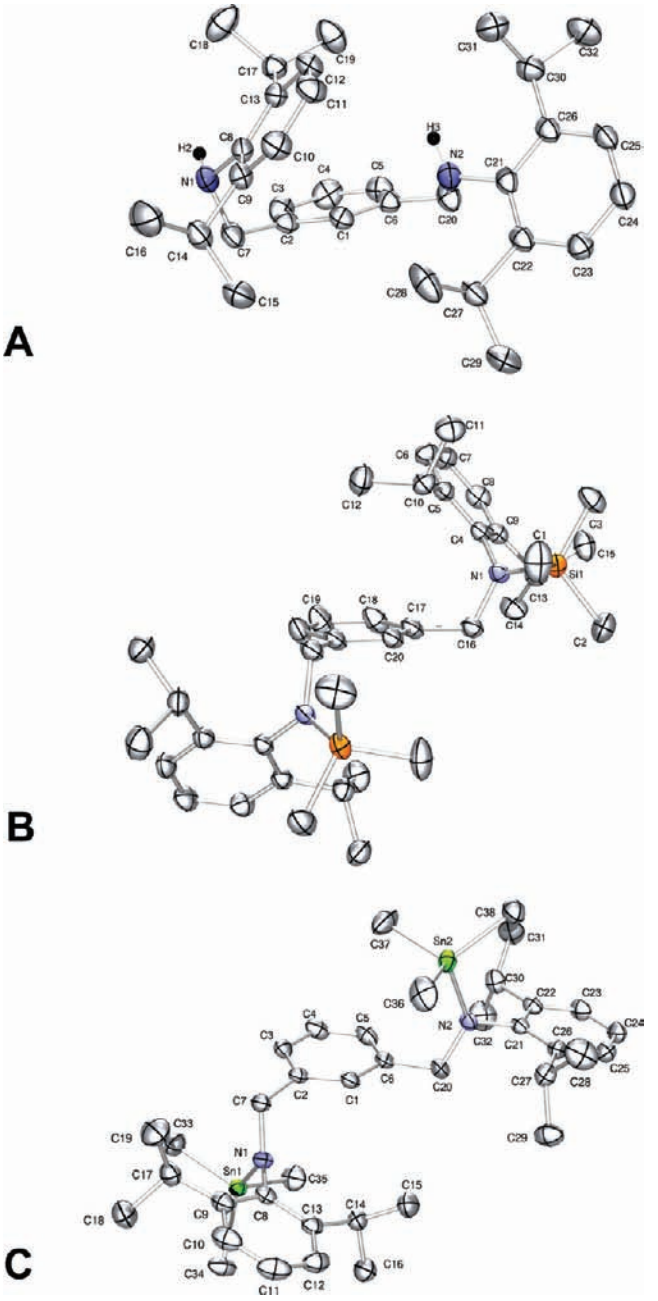

Figure 2. Ortep drawings of the molecular structure of (**A**) [2,6-^{i}PrNCN]H_3 (**8**), (**B**) [2,6-^{i}PrNCHN](SiMe$_3$)$_2$ (**9-Si**), and (**C**) [2,6-^{i}PrNCHN](SnMe$_3$)$_2$ (**9-Sn**) with ellipsoids presented at the 50% probability level and hydrogen atoms removed for clarity.

contains a complete list of bond lengths and angles. The asymmetric unit of **9-Si** consists of half a molecule, whereas **9-Sn** contains the entire molecule. The key features that distinguish the two compounds are the orientation of the **M**Me$_3$ and the N−**M** bond distances. In **9-Si**, both $SiMe_3$ groups orient toward one side of the molecule and possess a N−Si bond length of 1.7333(12) Å. For **9-Sn**, the $SnMe_3$ groups are anti, and the N−Sn bond length is appropriately longer at 2.0525(17) Å. In compounds **8**, **9-Si**, and **9-Sn**, the spatial location of the pendant arms is dependent on the N-substituent and the N−**M** bond length. In [2,6-^{i}PrNCN]H_3 (**8**) the centroid of the ^{i}Pr-aryl rings separate by approximately 6.35 Å, in [2,6-^{i}PrNCHN](SiMe$_3$)$_2$ (**9-Si**) by 9.58 Å, and in

Table 1. X-ray Crystallographic Structure Parameters and Refinement Data

	8	9-Si	9-Sn	12	13	16
empirical formula	$C_{32}H_{44}N_2$	$C_{19}H_{30}NSi$	$C_{38}H_{60}N_2Sn_2$	$C_{40}H_{58}Cl_2Mg_2N_2O_2$	$C_{64}H_{84}N_4Zn_2$	$C_{26}H_{20}F_{12}N_2$
formula weight	456.69	300.53	782.26	718.40	1040.09	588.44
crystal system	triclinic	monoclinic	monoclinic	monoclinic	monoclinic	triclinic
space group	$P\bar{1}$	$C2/c$	$P2(1)/c$	$P2_1/n$	$P2(1)/c$	$P\bar{1}$
crystal dimensions (mm)	0.20 × 0.18 × 0.05	0.26 × 0.15 × 0.09	0.15 × 0.13 × 0.12	0.15 × 0.11 × 0.07	0.31 × 0.26 × 0.20	0.11 × 0.08 × 0.05
a (Å)	10.7730(15)	17.3753(2)	13.0126(6)	14.1942(13)	43.169(7)	11.9159(14)
b (Å)	11.3453(16)	8.7733(5)	20.1984(10)	19.6408(18)	14.132(2)	14.003(2)
c (Å)	13.5349(19)	24.6156(14)	14.9236(7)	16.2155(15)	19.314(3)	16.6156(18)
α (deg)	112.047(2)	90	90	90	90	75.343(2)
β(deg)	90.730(2)	92.947(2)	101.7060(10)	113.689(2)	90.577(3)	71.727(2)
γ (deg)	113.013(2)	90	90	90	90	74.212(2)
volume (Å^3)	1386.4(3)	3747.0(4)	3840.8(3)	4139.7(7)	11782(3)	2490.3(5)
Z (Å)	2	8	4	4	8	4
absorption coeff (mm^{-1})	0.063	0.121	1.326	0.221	1.855	0.156
F (000)	500	1320	1608	1544	4448	1192
D_{calcd} (g/cm^3)	1.094	1.065	1.353	1.153	1.173	1.570
γ (Mo Kα) (Å)	0.71073	0.71073	0.71073	0.71073	0.71073	0.71073
Temperature (K)	173(2)	173(2)	173(2)	173(2)	100(2)	173(2)
θ range (deg)	2.09 to 27.49	1.66 to 27.49	1.60 to 27.50	1.62 to 27.50	0.94 to 27.50	1.31 to 22.50
completeness to θ_{max}	95.6%	98.0%	99.6%	98.7	99.4%	99.8%
reflections collected	9182	11752	25592	26976	84071	10886
indep reflections [R_{int}]	6079 [0.0503]	4227 [0.0317]	8782 [0.0404]	9382 [0.1544]	26885 [0.0361]	6488 [0.1286]
data/restraints/param	6079/0/315	4227/0/191	8782/0/379	9382/0/430	26885/0/1293	6488/0/890
final R_1 indices [$I > 2\sigma(I)$]	R1 = 0.0489, wR2 = 0.1213 [4187]	R1 = 0.0414, wR2 = 0.1041 [3473]	R1 = 0.0251, wR2 = 0.0616 [7781]	R1 = 0.0669, wR2 = 0.1601 [4900]	R1 = 0.0378, wR2 = 0.0912 [20900]	R1 = 0.0633, wR2 = 0.1387 [3149]
R indices (all data)	R1 = 0.0757, wR2 = 0.01347	R1 = 0.0530, wR2 = 0.1117	R1 = 0.0302, wR2 = 0.0636	R1 = 0.1429, wR2 = 0.1943	R1 = 0.0553, wR2 = 0.1000	R1 = 0.1350, wR2 = 0.1701
largest diff peak/ hole e.Å^{-3}	0.235/-0.209	0.300/-0.253	0.590/-0.398	0.391/-0.415	0.909/ −0.544	0.310/-0.263
goodness of fit on F^2	1.042	1.022	1.025	1.004	1.015	0.896

[2,6-^{i}PrNCHN](SnMe$_3$)$_2$ (**9-Sn**) by 10.2 Å. Though oriented differently in the solid-state, ^{1}H NMR spectroscopy indicates the −CH$_2$N**M**C$_6$H$_3$(^{i}Pr)$_2$ groups freely rotate in solution.

[2,6-^{i}PrNCHN](μ-MgCl·THF)$_2$ (12) and {[2,6-^{i}PrNCHN]Zn}$_2$ (13). Unlike the smooth synthesis of {[2,6-^{i}PrNCN]Li$_3$}$_2$ (**11**)[1] with MeLi, refluxing [2,6-^{i}PrNCN]H$_3$ (**8**) in toluene with 3 equiv of MeMgCl only provides intractable mixtures. The dimer of compound **11** contains a compact hexalithio core with no solvent molecules.[1] However, addition of 2 equiv of MeMgCl to **8** in THF results in formation of [2,6-^{i}PrNCHN](μ-MgCl·THF)$_2$ (**12**) in 89% yield as a microcrystalline powder (eq 2).

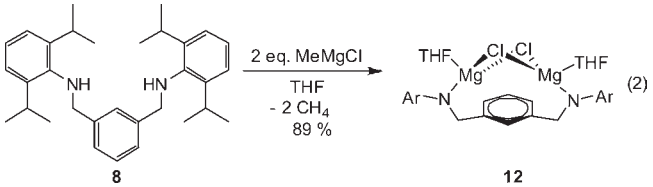

8 **12**

Figure 3 presents the results of a single-crystal X-ray diffraction experiment for **12**, and Table 1 lists crystallographic information. The salt contains a Mg$_2$Cl$_2$ core. Each Mg(II) ion completes its coordination sphere with a THF and one amido connection to the ligand, which chelates the core. Within the series of (**9-Si**), (**9-Sn**), (**10**), and (**12**), compound **12** is the only derivative to contain a single NCN fragment that chelates the cations. The bridging chlorides are the obvious cause for this observation, providing a stable diamond core.

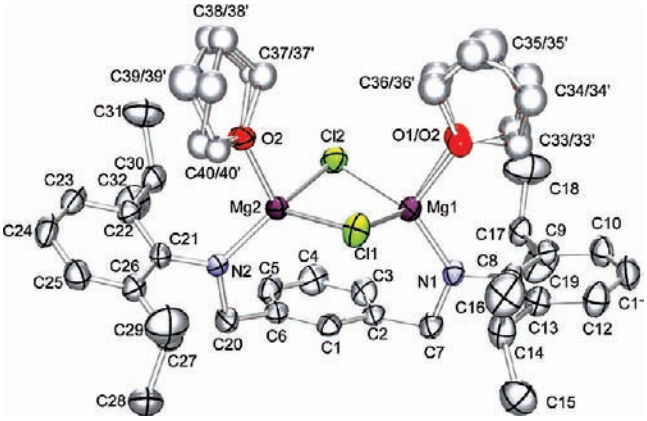

Figure 3. Thermal ellipsoid (50% probability) drawing of the molecular structure of [2,6-^{i}PrNCHN](μ-MgCl·THF)$_2$ (**12**) with hydrogen atoms removed for clarity. Coordinated THF molecules are disordered and their atoms (except O2) are refined isotropically. Selected bond lengths (Å) and angles (deg): Mg1−N1, 1.947(3); Mg1−O1, 2.004(5); Mg1−Cl1, 2.4162(14); Mg1−Cl2, 2.3911(14); Mg2−N2, 1.941(3); Mg2−O2, 2.015(2); Mg2−Cl1, 2.3939(14); Mg2−Cl2, 2.3851(13); Mg1−Cl1−Mg2, 94.58(5); Cl1−Mg2−Cl2, 92.78(5); Mg2−Cl2−Mg1, 85.32(5); Cl2−Mg1−Cl1, 92.07(5).

The ambient temperature ^{1}H NMR (C$_6$D$_6$) spectrum of **12** is misleading and is not representative of a chelating NCN fragment. The methylene protons on the NCN arms are equivalent and appear as a broad singlet at 4.44 ppm, which overlaps with the methine septet. The isopropyl methyls appear as two doublets (J = 6.0 Hz) at 1.48 and 1.30 ppm. The solid-state structure indicates the methylene protons must be diastereotopic, and each

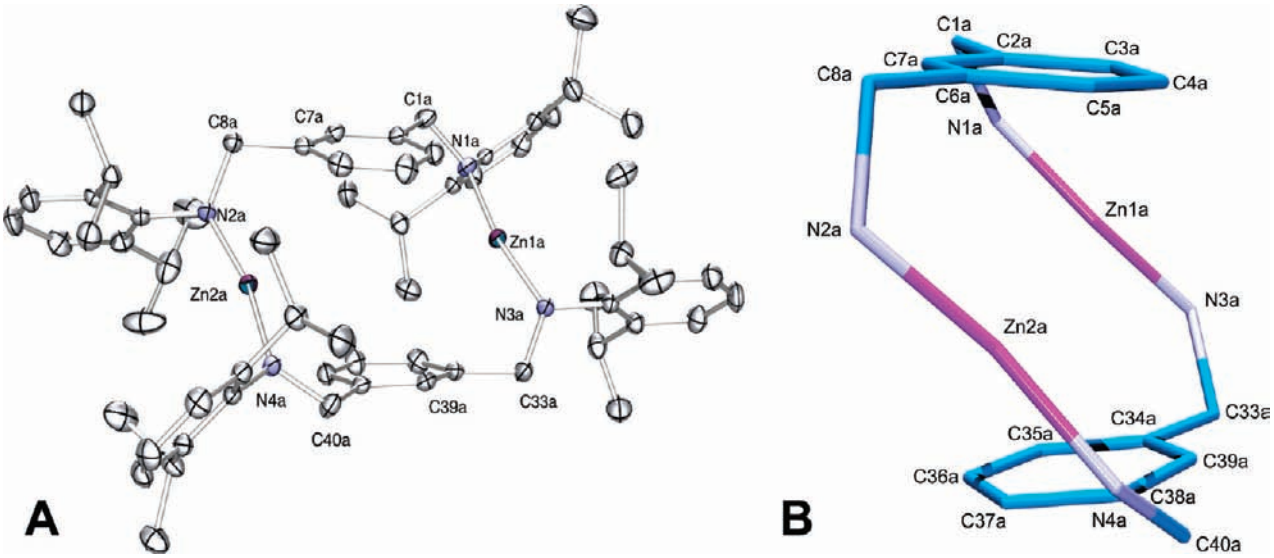

Figure 4. (**A**) Ortep drawings of the molecular structure of $\{[2,6\text{-}^{i}PrNCHN]Zn\}_2$ (**13**) with ellipsoids drawn at the 50% probability level and hydrogens removed for clarity. (**B**) Truncated view of **13** highlighting the two-coordinate Zn ions and the 16-membered Z-shaped metallocyle. Selected bond lengths (Å) and angles (deg): Zn1a−N1a, 1.8100(15); Zn1a−N3a, 1.8119(15); Zn2a−N2a, 1.8161(15); Zn2a−N4a, 1.8141(15); N1a−Zn1a−N3a, 164.65(7); N4a−Zn2a−N2a, 166.64(7).

Scheme 1

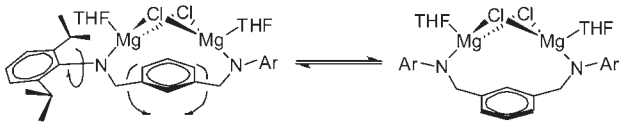

isopropyl methyl is unique, thus fluxional processes must equilibrate them. Rotation around the N−aryl bond explains the observation of two doublets instead of four for the ^{i}Pr methyls. However, to equilibrate the methylene protons the arene ring of the ligand must flip between two equivalent conformers (Scheme 1). Variable temperature (25 to −60 °C) ^{1}H NMR (toluene-d_8) experiments failed to quench these dynamic processes. The unlikely alternative mechanism requires cleavage of two μ-Mg−Cl bonds, followed by rotation around the N−CH_2 bond, and reattachment.

Anhydrous $ZnCl_2$ reacts with $\{[2,6\text{-}^{i}PrNCHN]Li_2\}_2$ (**10**)[15] to provide $\{[2,6\text{-}^{i}PrNCHN]Zn\}_2$ (**13**) in 68% yield (eq 3). A single crystal X-ray diffraction experiment confirms the bimetallic composition of **13** and reveals each Zn ion is two-coordinate. Figure 4A displays the molecular structure of **13**, and a truncated picture highlighting the 16-member metallocycle and its Z-shape conformation (Figure 4B).

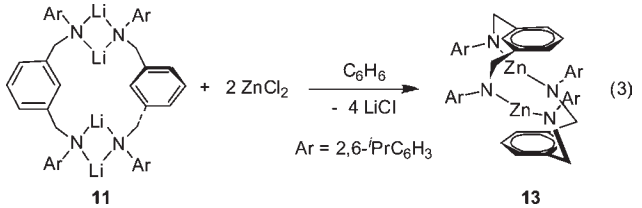

11 **13**

Crystallographic data is found in Table 1, and the Supporting Information contains a complete list of bond lengths and angles. The asymmetric unit consists of two crystallographically independent bimetallic units in which one dimer resides in a general position, and two halves reside on inversion centers. The Zn(II) ions are two coordinate creating a nearly linear geometry between two ligand molecules (N−Zn−N_{avg} = 164.86(7)°). The closest contacts are all greater than 3 Å from the Zn ions. Structural details of two coordinate Zn-amido complexes are scarce[19] owing to a preference to dimerize.[20] Compound **13** is unique because it combines two, two coordinate Zn(II) ions within the same compound. The average Zn−N bond length is 1.8116(5) Å, which is much shorter than the sum of covalent radii (2.13 Å) and consistent with other short Zn−N bonds which involve Np_π to Znp_π bonding in $Zn[N(SiMePh_2)_2]_2$ (1.824(14) Å),[19e] $Zn[N(SiMe_3)(SiPh_2{}^{t}Bu)]_2$ (1.853(2) and 1.858(2) Å),[19a] Zn[N(SiMe$_3$)(Ad)] (1.827(2) and 1.828(14) Å),[19a] $Zn[N(SiMe_3)(^{t}Bu)]_2$ (1.82 Å),[19d] and $Zn[N(SiMe_3)_2]_2$ (1.82 Å, by gas phase electron diffraction).[19f] Clearly, the short bond distance is due to Np_π to Znp_π bonding. To maximize π-donation the local environment of each N-atom twists along the N−Zn−N axis, creating dihedral angles of 57° and 55° between planes created by the three N-atom substituents.

Figure 5 is a space-filling representation of **13** and indicates the Zn ions are protected by the arene rings and the isopropyl groups. However, **13** reacts instantaneously with H_2O to form $[2,6\text{-}^{i}PrNCN]H_3$ (**8**)[15] and

(19) (a) Tang, Y. J.; Felix, A. M.; Boro, B. J.; Zakharov, L. N.; Rheingold, A. L.; Kemp, R. A. *Polyhedron* **2005**, *24*, 1093–1100. (b) Schumann, H.; Gottfriedsen, J.; Dechert, S.; Girgsdies, F. *Z. Anorg. Allg. Chem.* **2000**, *626*, 747–758. (c) Gaul, D. A.; Just, O.; Rees, W. S. *Inorg. Chem.* **2000**, *39*, 5648–5654. (d) Rees, W. S.; Green, D. M.; Hesse, W. *Polyhedron* **1992**, *11*, 1697–1699. (e) Power, P. P.; Ruhlandtsenge, K.; Shoner, S. C. *Inorg. Chem.* **1991**, *30*, 5013–5015. (f) Haaland, A.; Hedberg, K.; Power, P. P. *Inorg. Chem.* **1984**, *23*, 1972–1975. (g) Burger, H.; Sawodny, W.; Wannagat, U. *J. Organomet. Chem.* **1965**, *3*, 113–&.

(20) (a) Armstrong, D. R.; Forbes, G. C.; Mulvey, R. E.; Clegg, W.; Tooke, D. M. *J. Chem. Soc., Dalton Trans.* **2002**, 1656–1661. (b) Just, O.; Gaul, D. A.; Rees, W. S. *Polyhedron* **2001**, *20*, 815–821. (c) Putzer, M. A.; Dashti-Mommertz, A.; Neumuller, B.; Dehnicke, K. *Z. Anorg. Allg. Chem.* **1998**, *624*, 263–266. (d) Schumann, H.; Gottfriedsen, J.; Girgsdies, F. *Z. Anorg. Allg. Chem.* **1997**, *623*, 1881–1884.

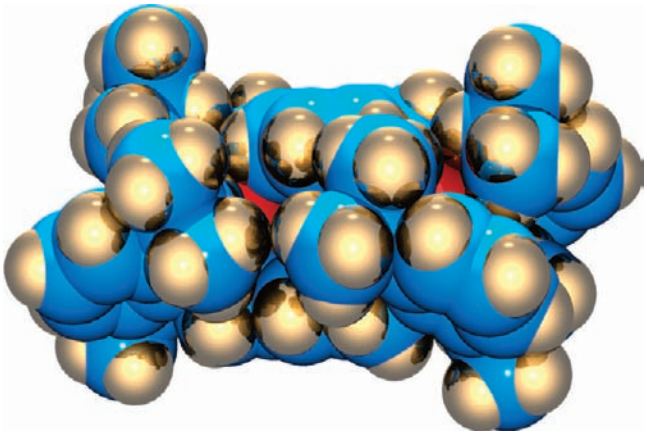

Figure 5. Space-filling drawing of the molecular structure of {[2,6-^{i}PrNCHN]Zn}$_2$ (**13**).

$Zn(OH)_2$, implying easy access to the Zn ions. Compound **13** exhibits an ambient temperature ^{1}H NMR(C_6D_6) spectrum consistent with the formula [2,6-^{i}PrNCHN]Zn, but not the solid-state structure. Broad singlets appear at 1.24 and 4.23 ppm for the isopropyl methyl and methylene protons, respectively. The methine protons appear as a broadened septet at 3.91 ppm. The solid-state structure indicates the methylene protons should be diastereotopic.

A variable temperature ^{1}H NMR (toluene-d_8) experiment indicates a fluxional process occurs, and at −60 °C the isopropyl methyl protons resolve into two doublets at 1.04 and 1.34 ppm. The coalescence temperature occurs at −10 °C corresponding to an activation energy of $\Delta G^{\ddagger} =$ 12.6(3) kcal/mol. The resolution of the isopropyl groups into two distinct signals is due to restricted rotation around the N−aryl bond. However, even at −60 °C a rapid dynamic process still occurs; the methylene groups still appear as a singlet. Low solubility in hydrocarbon and aromatic solvent prevents analysis at temperatures below −60 °C. Scheme 2 depicts a plausible mechanism for the methylene group coalescence. Compound **13** can adopt either open or closed conformations. When closed, the compound is C_{2h}-symmetric, providing two distinct environments for the methylene protons. When open, the symmetry is D_{2h}, and the protons become equivalent.

[3,5-CF$_3$N^{C}C^{C}N]H$_3$ (16) and [3,5-CF$_3$N^{C}CH^{C}N](SiMe$_3$)$_2$ (17). We sought a two-carbon arm pincer ligand precursor. Raney-Nickel catalyzed reduction of 2,2′-benzene-1,3-diyldiacetonitrile (**14**) (90 atm H_2, NH_3 saturated MeOH, 90 °C) provides 2,2′-benzene-1,3-diyldiethanamine (**15**) in 80% yield.[18] For convenience, the reduction may be accomplished with $LiAlH_4$ in Et_2O,[21] but provides **15** in only 39% yield after purification by vacuum distillation. Cross-coupling[22] between **15** and 3,5-trifluoromethylbromobenzene produces *N*,*N*′-(1,3-phenylenebis(methylene))bis(3,5-bis(trifluoromethyl)aniline) [3,5-CF$_3$N^{C}C^{C}N]H$_3$ (**16**) in 33% yield as a colorless microcrystalline powder after two recrystallizations (eq 4).[23] A ^{1}H NMR (C_6D_6) spectrum of **16** reveals two sets of resonances for the methylene protons as a doublet of triplets at 2.73 ppm ($J = 6.0$ Hz and $J = 6.0$ Hz; -CH_2CH_2NH-) and a triplet at 2.38 ppm ($J = 6.0$ Hz; -CH_2CH_2NH-). The NH proton resonates as a triplet ($J = 6.0$ Hz) at 3.13 ppm.

Scheme 2

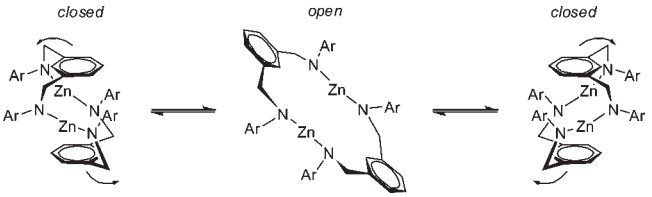

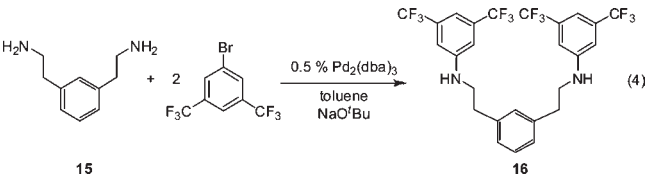

Single crystals grow from a saturated Et_2O solution of **16** at −35 °C, and Figure 6A depicts its solid-state molecular structure determined from an X-ray diffraction experiment. Crystallographic data is found in Table 1, and the Supporting Information contains a complete list of bond lengths and angles. The asymmetric unit consists of two crystallographically unique molecules that connect through a triple arene π-stacking interaction. Two of the trifluoroaryl groups from one molecule wrap around a single arene group of the other. Figure 6B depicts the π-stacking relationship and highlights the approximately 3.84 Å and 3.78 Å separations between the centroids of the arene planes. To accommodate the trifuoro groups, the central ring staggers between the two outer rings creating torsion angles between CF_3 groups of 37° and 44°; however, the two outer rings are nearly eclipsed ($\angle$C24−C15−C21−C23 ≈ 7°). Presumably the π-stacking and triflouro groups impart significant crystallinity to **16** because the mesityl derivative [MesN^{C}C^{C}N]-H_3 is a viscous oil.[24]

Previous success at metalating the NCN trilithio salt {[2,6-^{i}PrNCN]Li$_3$}$_2$ (**11**)[1] with group 4 ions prompted attempts to synthesize {[3,5-CF$_3$N^{C}C^{C}N]Li$_3$}$_2$. However, deprotonation with RLi (R = ^{t}Bu, Bu, Me) results in lithiation of multiple sites, including the methylene groups. As a consequence, other metalation strategies were sought. Treating **16** with MeMgCl followed by excess Me_3SiCl provides [3,5-CF$_3$N^{C}CH^{C}N](SiMe$_3$)$_2$ (**17**) in 74% yield as a crystalline white solid (eq 5).

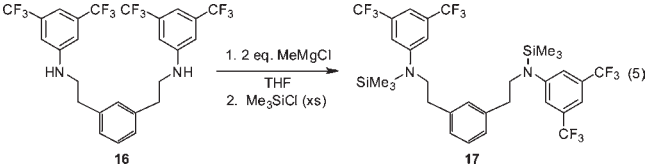

A ^{1}H NMR (C_6D_6) spectrum of **17** confirms the Me_3Si-substitution. Removal of the N−H proton reduces the

(21) Cummins, C. C.; Beachy, M. D.; Schrock, R. R.; Vale, M. G.; Sankaran, V.; Cohen, R. E. *Chem. Mater.* **1991**, *3*, 1153–1163.

(22) (a) Guram, A. S.; Buchwald, S. L. *J. Am. Chem. Soc.* **1994**, *116*, 7901–7902. (b) Paul, F.; Patt, J.; Hartwig, J. F. *J. Am. Chem. Soc.* **1994**, *116*, 5969–5970. (c) Guram, A. S.; Rennels, R. A.; Buchwald, S. L. *Angew. Chem., Int. Ed. Engl.* **1995**, *34*, 1348–1350. (d) Louie, J.; Hartwig, J. F. *Tetrahedron Lett.* **1995**, *36*, 3609–3612. (e) Driver, M. S.; Hartwig, J. F. *J. Am. Chem. Soc.* **1996**, *118*, 7217–7218. (f) Wolfe, J. P.; Rennels, R. A.; Buchwald, S. L. *Tetrahedron* **1996**, *52*, 7525–7546. (g) Wolfe, J. P.; Wagaw, S.; Marcoux, J. F.; Buchwald, S. L. *Acc. Chem. Res.* **1998**, *31*, 805–818.

(23) (a) Wolfe, J. P.; Buchwald, S. L. *J. Org. Chem.* **2000**, *65*, 1144–1157. (b) Wolfe, J. P.; Wagaw, S.; Buchwald, S. L. *J. Am. Chem. Soc.* **1996**, *118*, 7215–7216.

(24) Carlson, A. R. MSc. Thesis, University of Florida, Gainesville, FL, **2007**.

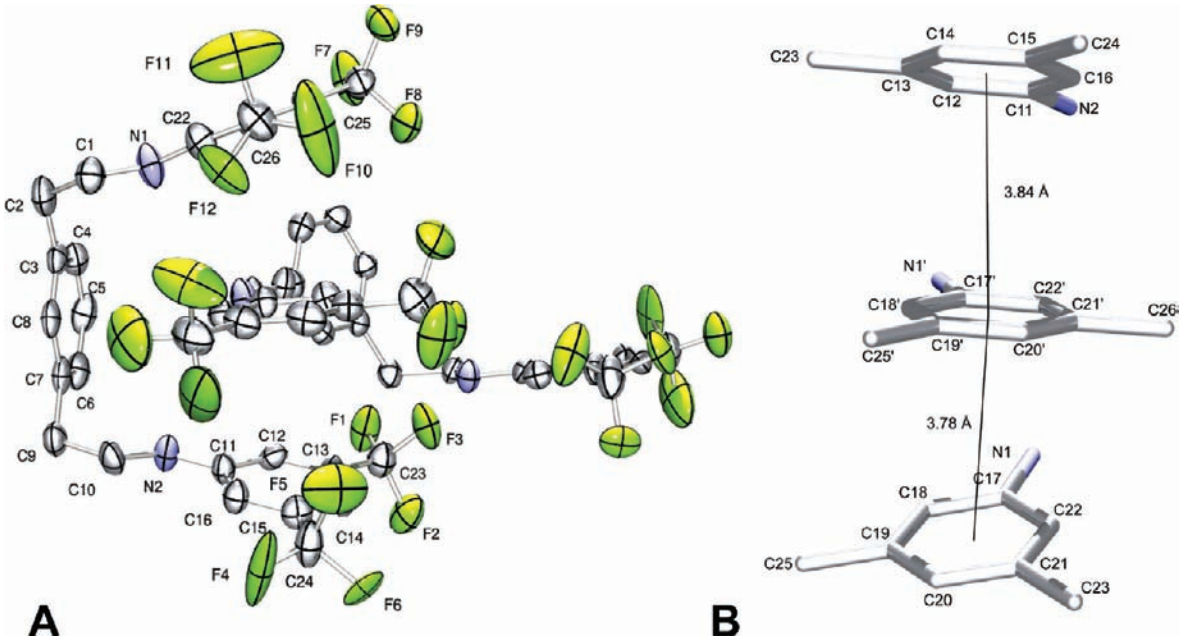

Figure 6. (**A**) Ortep drawing of the molecular structure of [3,5-$CF_3N^CC^CN$]H_3 (**16**) with ellipsoids presented at the 50% probability level. (**B**) Truncated drawing of **16** highlighting the π-stacking between two molecules in the asymmetric unit.

doublet of triplets in **16** to a triplet for **17** at 3.23 ppm ($J = 6.0$ Hz) and the Me_3Si protons resonate at 0.00 ppm. The $^{13}C\{^1H\}$ NMR (C_6D_6) spectrum is complementary and reveals a resonance at 0.7 ppm for the (CH_3)$_3$Si-carbons and quartet at 132.8 ppm for the CF_3 groups (q, $J = 32.2$ Hz). Additional aliphatic (35.6 ppm (s, -CH_2−Ar), 49.0 ppm (s, -CH_2N)) and aromatic resonances (between 112.3 and 150.8 ppm) complete the assignment.

[3,5-$CF_3N^CC_{anth}{}^CN$]H_3 (18). A more rigid ligand is the anthracene derivative [3,5-$CF_3N^CC_{anth}{}^CN$]H_3 (**18**). Pale yellow **18** forms by combining bis(bromomethylene)-anthracene,[16,25] 3,5-triflouroaniline, and K_2CO_3 and stirring for 12 h in DMF (eq 6). Purification by flash column chromatography (1:1 $CHCl_3$:pentane) provides **18** in 46% yield. ^1H, ^{13}C NMR (C_6D_6) spectroscopy and mass spectrometry confirm the identity of **18**. The ^1H NMR spectrum reveals a distinct doublet for the CH_2 group at 4.01 ppm ($J = 5.0$ Hz) which couples to the NH proton, appearing at 3.24 ppm ($J = 5.0$ Hz). Other noteworthy resonances include a singlet for the four *o*-CH protons at 6.47 ppm and two singlets at 8.32 and 8.24 ppm for the opposing CH protons on the central arene ring of the anthracene. Appropriate ^{13}C NMR resonances appear for the aromatic carbons of **18**, but distinct signals appear for the CH_2 and CF_3 carbons at 46.8 ppm and 110.9 ppm, respectively, the latter being slightly broadened.

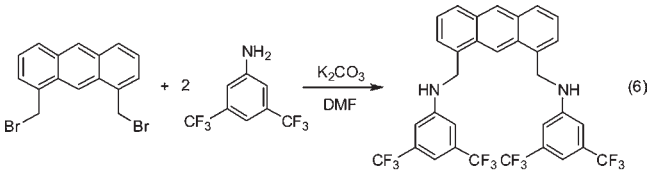

18

Synthesis and Characterization of Group 4 NCN Complexes. Direct metalation of the parent NCN ligands [2,6-^{i}PrNCN]H_3 (**8**) and [3,5-$CF_3N^CC^CN$]H_3 (**16**) with MCl_4 or $MCl_4(THF)_2$ (M = Ti, Zr, and Hf) and pyridine (as an HCl sponge) does not result in M-ligand bond formation. McConville et al. metalated $TiCl_4$ with the disilyamide ligand precursor N^1,N^3-bis(2,6-diisopropylphenyl)-N^1,N^3-bis(trimethylsiliyl)propane-1,3-diamine in refluxing toluene.[26] (**9-Si** and **17**) and (**9-Sn**) ligand precursors offer a chance to first chelate through the amido linkages via Me_3SiCl and Me_3SnCl elimination.[27] Subsequent arene C−H bond activation would provide a trianionic ligand. However, refluxing **9-Si**, **9-Sn**, or **17** in the presence of MCl_4 salts either provides intractable mixtures or no reaction (eq 7).

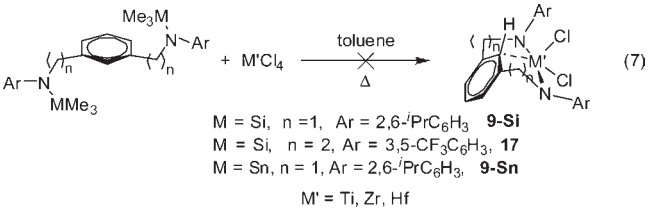

{(μ-3,5-$CF_3N^CCH^CN$)Zr(NMe_2)$_2$NHMe_2}$_2$ (19). Direct metalation with the parent diamine ligands is the most convenient method to produce trianionic pincer ligand complexes. Reasonable transition metal substrates are homoleptic metal-amido and metal−alkyl complexes. This method works with Mo(NMe_2)$_4$ and the terphenyl diphenolate ligand, but the terphenyl framework seems to be key, and this is not a general reaction. For instance, Lappert et al. report the synthesis of the dinuclear

(25) (a) Akiyama, S.; Misumi, S.; Nakagawa, M. *Bull. Chem. Soc. Jpn.* **1960**, *33*, 1293–1298. (b) House, H. O.; Koepsell, D.; Jaeger, W. *J. Org. Chem.* **1973**, *38*, 1167–1173.

(26) Scollard, J. D.; McConville, D. H.; Vittal, J. J.; Payne, N. C. *J. Mol. Catal. A: Chem.* **1998**, *128*, 201–214.

(27) Morrison, D. L.; Rodgers, P. M.; Chao, Y. W.; Bruck, M. A.; Grittini, C.; Tajima, T. L.; Alexander, S. J.; Rheingold, A. L.; Wigley, D. E. *Organometallics* **1995**, *14*, 2435–2446.

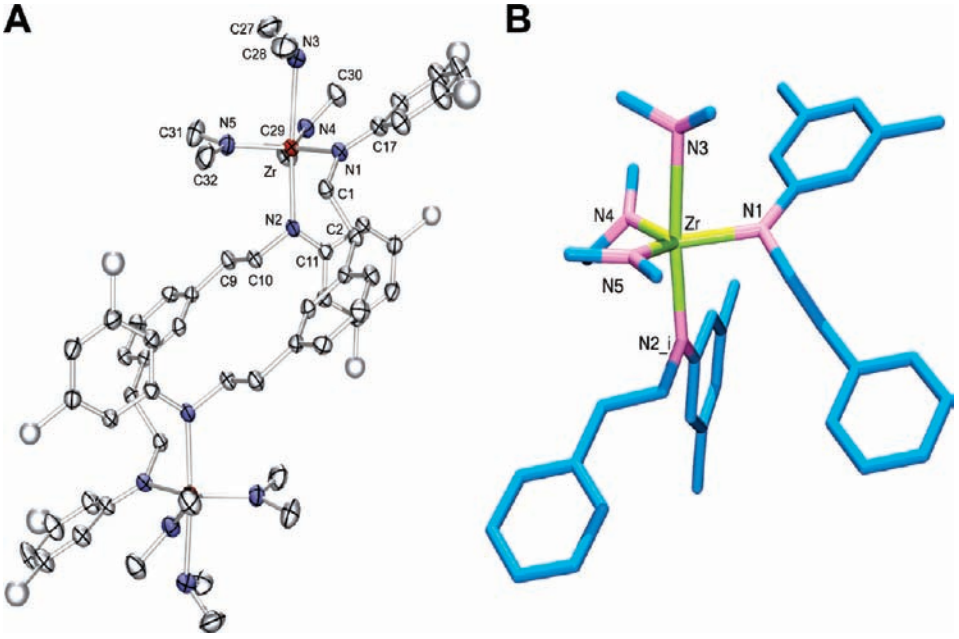

Figure 7. (**A**) Ortep drawing of the molecular structure of $\{(\mu\text{-}3,5\text{-}CF_3N^CCH^CN)Zr(NMe_2)_2NHMe_2\}_2$ (**19**) with ellipsoids presented at the 50% probability level and hydrogen and fluorine atoms removed for clarity. (**B**) Truncated drawing of **19** highlighting the trigonal bipyramidal Zr core. Selected bond lengths (Å) and angles (deg): Zr−N1, 2.137(2); Zr−N2_i, 2.212(2); Zr−N3, 2.461(3); Zr−N4, 2.036(3); Zr−N5, 2.037(3); C28−N3−C27, 109.4(3); N3−Zr−N2_i = 174.00(10); N4−Zr−N5, 114.44(11); N4−ZR−N1, 122.10(10); N5−Zr−N1, 121.45(10).

complex $[\mu\text{-}2,6\text{-}^i\text{PrNCHN}]\{Zr(NMe_2)_3\}_2$ from $[2,6\text{-}^i\text{PrNCN}]H_3$ (**8**) and $\{Zr(NMe_2)_4\}_2$.[15a]

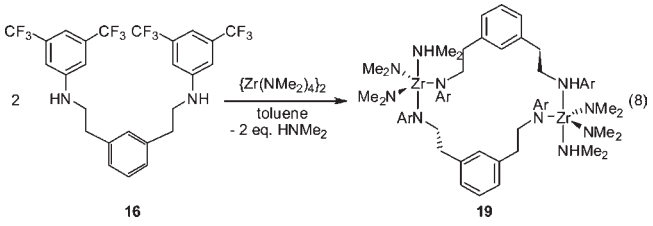

Using the extended-arm ligand precursor **16** and $\{Zr(NMe_2)_4\}_2$ provides a similar result. The dimer $\{(\mu\text{-}3,5\text{-}CF_3N^CCH^CN)Zr(NMe_2)_2NHMe_2\}_2$ (**19**) forms by treating $\{Zr(NMe_2)_4\}_2$ with **16** in toluene first at −35 °C followed by stirring at ambient temperature for 3 h (eq 8). Figure 7 displays the results of an X-ray diffraction experiment performed on single-crystals of **19** grown from a saturated benzene solution. Table 2 lists refinement data. The complex consists of two trigonal bipyramidal Zr(IV) ions bridged by two N^CC^CN ligands. Each Zr contains four amido connections; two from the bridging NCN ligand and two from NMe_2 groups. A fifth site, (axial) contains one $HNMe_2$ ligand produced in the aminolysis reaction. The asymmetric unit contains half the dimer and a benzene molecule. Because of disorder within the CF_3 groups, each F-atom requires refinement over three positions to total site occupancy of one. The Zr−N bond lengths span a difference of 0.4 Å. The longest Zr−N bond length (d(Zr−N3) = 2.461(3) Å) is appropriate for the Zr-amine connection, and the two shortest are from the Zr-NMe_2's (d(Zr−N4) = 2.036(3) Å and d(Zr−N5) = 2.037(3) Å). Intermediate (d(Zr−N1) = 2.137(2) Å and d(Zr−N2_i) = 2.212(2) Å) bond lengths form with the NCN amido connection and may be due to the slightly less π-basic character of the aryl-amide versus alkyl-amide.

The obvious difference between the dinuclear species produced from $[2,6\text{-}^i\text{PrNCN}]H_3$ (**8**) and $[3,5\text{-}CF_3N^CC^CN]H_3$ (**16**) and $\{Zr(NMe_2)_4\}_2$ is one contains a single bridging ligand and one contains two. The more flexible, extended-arm ligand comfortably spans two metals centers, though neither produces a trianionic ligand bound complex. An attempt to activate the aryl C−H bond in the central ring by refluxing **19** in toluene results in no detectable reaction.

(μ-3,5-$CF_3N^CCH_{anth}{}^CN$){$Hf(NMe_2)_3NHMe_2$}$_2$ (20). If a too-flexible ligand provides dinuclear species, then the more rigid anthracene derivative $[3,5\text{-}CF_3N^CC_{anth}{}^CN]H_3$ (**18**) may promote chelation. Another possibility is the dinuclear composition of metal-precursor $\{Zr(NMe_2)_4\}_2$ is the cause of dimer formation, not the ligand. However, even the presumably more rigid **18** produces a dinuclear complex, albeit with only one bridging ligand, from the mononuclear metal source $Hf(NMe_2)_4$. Treatment of **18** with 2 equiv of $Hf(NMe_2)_4$ in benzene results in the formation of pale yellow (μ-3,5-CF_3 $N^CCH_{anth}{}^CN$){$Hf(NMe_2)_3NHMe_2$}$_2$ (**20**) (eq 9). The reaction is complete within 10 min at room temperature, but **20** precipitates from the reaction medium after 1 h. Using 1 equiv of $Hf(NMe_2)_4$ only results in reduced conversion. A combination of ^{1}H and ^{13}C NMR (C_6D_6) spectroscopy, combustion analysis, and an X-ray diffraction study confirms the identity of **20**.

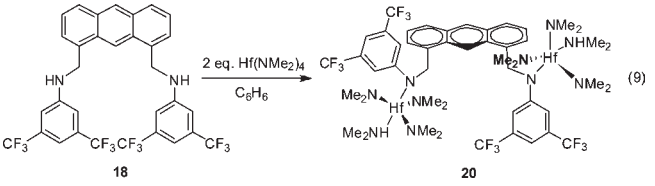

Single crystals amenable to an X-ray diffraction experiment grow by pentane diffusion into a diethyl ether

Table 2. X-ray Crystallographic Structure Parameters and Refinement Data

	19	**20**	**21**	**23**
empirical formula	$C_{76}H_{86}F_{24}N_{10}Zr_2$	$C_{48}H_{68}F_{12}N_{10}Hf_2$	$C_{36}H_{54}N_4Zr$	$C_{46}H_{77}Hf\,LiN_2O_6$
formula weight	1777.99	1370.10	634.05	939.53
crystal system	triclinic	monoclinic	triclinic	monoclinic
space group	$P\bar{1}$	$P2_1/c$	$P\bar{1}$	$P2(1)/n$
crystal dimensions (mm)	0.19 × 0.19 × 0.06	0.17 × 0.04 × 0.04	0.26 × 0.25 × 0.09	0.30 × 0.17 × 0.13
a (Å)	9.1226(5)	17.3997(11)	8.2682(14)	11.2841(13)
b (Å)	12.3882(7)	20.3795(12)	12.2632(16)	20.515(2)
c (Å)	18.5955(10)	15.9524(10)	18.800(4)	20.8(2)
α (deg)	77.615(1)	90	107.72(2)	90
β (deg)	79.183(1)	93.829(1)	91.20(2)	90.893(2)
γ (deg)	88.269(1)	90	108.229(19)	90
volume (Å^3)	2016.04(19)	6544.0(6)	1710.4(5)	4833(1)
Z (Å)	1	4	2	4
absorption coeff (mm^{-1})	0.362	3.757	0.231	2.203
F (000)	908	2712	676	1960
D_{calcd} (g/cm^3)	1.464	1.612	1.231	1.291
γ (Mo Kα) (Å)	0.71073	0.71073	0.71073	0.71073
temperature (K)	173(2)	173(2)	173(2)	100(2)
θ range (deg)	1.68 to 27.50	1.17 to 27.50	1.15 to 27.50	1.95 to 27.50
completeness to θ_{max}	94.9%	99.8%	94.9%	100.0%
reflections collected	13079	36722	12504	68129
indep reflections [R_{int}]	8784 [0.0386]	12966 [0.0962]	7445 [0.0148]	11108[0.0223]
data/restraints/param	8784/4/543	12966/4/697	7445/0/374	11108/0/521
final R_1 indices	R1 = 0.0537,	R1 = 0.0469,	R1 = 0.0337,	R1 = 0.0182,
[$I > 2\sigma(I)$]	wR2 = 0.1333 [7414]	wR2 = 0.583 [5882]	wR2 = 0.0950 [7081]	wR2 = 0.0443[10208]
R indices (all data)	R1 = 0.0638,	R1 = 0.1412,	R1 = 0.0353,	R1 = 0.0211,
	wR2 = 0.1398	wR2 = 0.0736	wR2 = 0.0966	wR2 = 0.0464
largest diff peak/hole e Å^{-3}	0.902/−0.778	1.643/−1.058	0.768/−0.732	1.116/−0.7631.131
goodness of fit on F^2	1.048	0.821	1.043	1.027

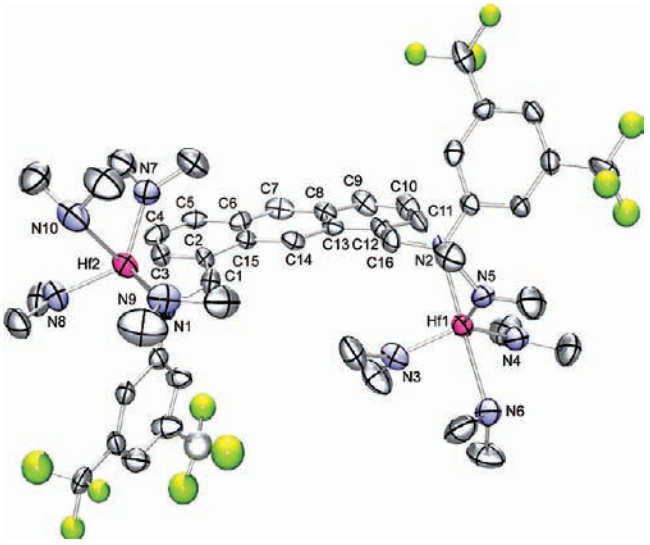

Figure 8. Ortep drawing of the molecular structure of (μ-3,5-$CF_3N^CCH_{anth}{}^CN$){Hf(NMe_2)$_3$$NHMe_2$}$_2$ (**20**) with ellipsoids presented at the 50% probability level and hydrogen atoms removed for clarity. Selected bond lengths (Å) and angles (deg): Hf1−N2, 2.188(5); Hf1−N3, 1.990(5); Hf1−N4, 2.032(6); Hf1−N5, 2.019(5); Hf2−N1, 2.185(5); Hf2−N6, 2.419(5); Hf2−N7, 1.992(5); Hf2−N8, 2.037(6); Hf2−N9, 2.032(6); Hf2−N10, 2.436(6); C2−C1−N1, 118.0(5); C12−C16−N2, 118.6(5); N2−Hf1−N6, 178.83(19); N1−Hf2−N10, 177.4(2).

solution of **20**. Figure 8 depicts the molecular structure of **20**, and Table 2 lists crystal and refinement data. The geometry of each hafnium ion is trigonal bipyramidal, and the overall symmetry of the compound is C_2-symmetric. One dimethylamine occupies the site trans to the NCN amide, and three dimethylamides occupy three equatorial sites. Average Hf−N bond lengths for the dimethylamides and ligand amides are 2.017(14) Å and 2.187(7) Å, respectively, and the Hf-$NHMe_2$ bond length is longer at 2.428(8) Å. Bond angles around the hafnium atom deviate slightly from the ideal trigonal bipyramidal values, with the average N−Hf−N angle for the equatorial dimethylamides being 119.2(5)°. The average N−Hf−N angle along the axis between the NCN amide and the dimethylamine is 178.1(3)°.

The ^{1}H NMR spectrum of **20** agrees with the solid-state analysis. One singlet at 2.59 ppm[26] appears for all the equatorial amido NMe's. The proton on the axial $NHMe_2$ ligand does not exchange, at least on the NMR time scale, with the other amido ligands. A distinct septet appears at 0.68 ppm (J = 6.3 Hz) for the N-*H* and the corresponding doublet (N-*Me*) appears at 1.52 ppm. Singlets for the central arene C-*H*'s resonate at 9.02 and 8.13 ppm. The proximity of hafnium to the C14 proton (see Figure 8) must deshield it downfield to 9.02 ppm. The ^{13}C{^{1}H} NMR spectrum of **20** further supports its assignment and matches the solid and solution state analysis. Thirteen aromatic resonances appear between 107.8 and 159.5 ppm, but the key signals resonate at 52.4, 42.3, and 39.3 ppm for the Ar*C*H_2N, Hf−N(*C*H_3)$_2$ and Hf-NH(*C*H_3)$_2$ carbons, respectively.

[2,6-^{i}PrNCHN]Zr(NMe_2)$_2$ (21). The metalation examples above all result in dinuclear complexes, and they all rely on aminolysis to attach the M−N bonds. Cleary, once one NCN M−N bond forms, the second arm reaches for a second metal. Reversible aminolysis will exacerbate this problem, especially with the more flexible ligands. An irreversible salt metathesis to first form the M−N bond prevents dimer formation. Treating Zr(NMe_2)$_2$$Cl_2$($THF$)$_2$[17] with {[2,6-^{i}PrNCHN]Li_2}$_2$ (**10**)[15a]

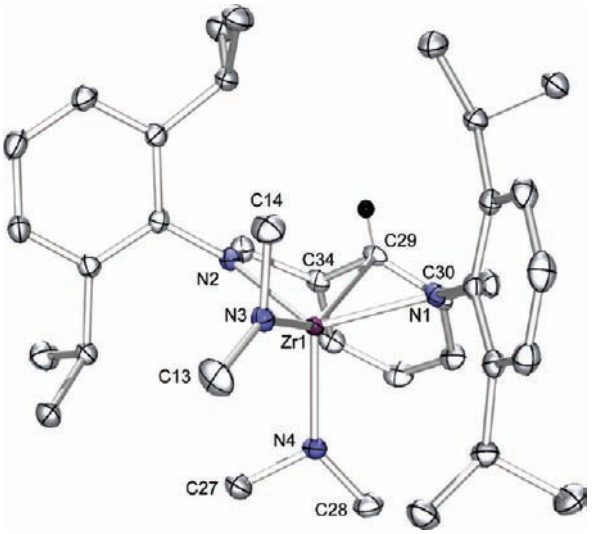

Figure 9. Ortep drawing of the molecular structure of [2,6-^{i}PrNCHN]-Zr(NMe$_2$)$_2$ (**21**) with ellipsoids presented at the 50% probability level and hydrogen atoms removed for clarity. Selected bond lengths (Å) and angles (deg): Zr1−N1, 2.1440(17); Zr1−N2, 2.1797(16); Zr1−N3, 2.0182(17); Zr1−N4, 2.0465(17); Zr1−C29, 2.6561(18); N1−Zr1−N2, 128.94(6); N1−Zr1−N4, 105.97(7); N2−Zr1−N4, 110.31(7); N3−Zr1−C29, 149.90(6); N1−Zr1−N3, 102.88(7); N2−Zr1−N3, 99.10; N3−Zr1−N4, 107.54(7); N4−Zr1−C29, 102.53(7).

provides the mononuclear complex [2,6-^{i}PrNCHN]Zr-(NMe$_2$)$_2$ (**21**) in 42% yield as a yellow microcrystalline powder (eq 10).

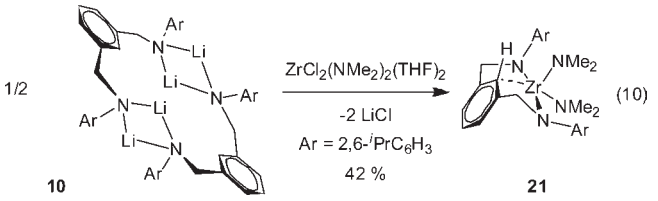

Single crystals grow at −35 °C from saturated pentane/ether solutions of **21**. Figure 9 depicts the results from an X-ray diffraction experiments performed on **21**, and Table 2 lists crystal and refinement data. [2,6-^{i}PrNCH-N]Zr(NMe$_2$)$_2$ (**21**) is pseudo C_s-symmetric with a highly distorted trigonal bipyramidal Zr center and a chelating diamido ligand.[26,28] The equatorial positions comprise the NCN amidos and a NMe$_2$ ligand, whereas the axis comprises a second NMe$_2$ and an agostic Zr−C$_{ipso}$ bond. The axis is significantly bent from linearity (∠N3−Zr1−C29 = 149.90(6)°) and the equatorial angle between the NCN amidos is splayed (∠N1−Zr1−N2 = 128.94(6)°). Consequently, two smaller angles form between the remaining equatorial positions (∠N1−Zr1−N4 = 105.97(7)° and N2−Zr1−N4 = 110.31(7)°). Clear indication of a Zr−C$_{ipso}$ interaction is evident by the short distance between the two atoms (d(Zr1−C29) = 2.6561(19) Å). The ^{1}H NMR (C$_6$D$_6$) spectrum of **21** provides additional information about the Zr−C$_{ipso}$ interaction and matches the C_s symmetry in the solid state. The CH_{ipso} proton appears well downfield at 9.34 ppm. More importantly, unlike in **12** above, the arene interaction is not fluxional. Four distinct doublets (J = 6.0 Hz) resonate at 1.42, 1.41, 1.35, and 1.24 ppm for each unique isopropoyl methyl. The corresponding septets for the methine CH's appear at 3.92 and 3.70 ppm. The NMe$_2$ ligands must freely rotate around the Zr−N bond because two singlets appear at 2.49 and 2.06 ppm, instead of four.

Despite the seemingly activated and position of the aryl-CH bond on the backbone, prolonged thermolysis of **21** in C$_6$D$_6$ at 90 °C and periodic examination by ^{1}H NMR spectroscopy indicates no reaction occurs (eq 11).

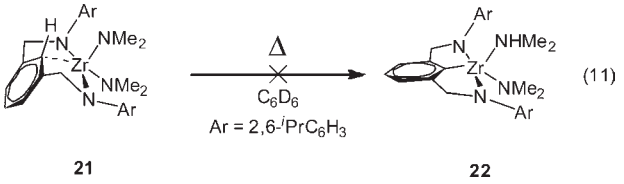

The equivalent activation is facile at ambient temperature for Mo(NMe$_2$)$_2$ and the OCO ligand derivative to form the bisamine complex [^{t}BuOCO]MoNMe$_2$(NHMe$_2$)$_2$ (**3**).[5,6] The anticipated NCN trianionic complex **22** may form, but the reaction is a reversible one in which the equilibrium heavily favors **21**. Addition of an equivalent of pyridine to potentially stabilize **22** did not lead to a reaction at 90 °C.

[2,6-^{i}PrNCNHfMe$_2$][Li(DME)$_2$] (23). Poor yields result when {[2,6-^{i}PrNCN]Li$_3$}$_2$ (**11**) and HfCl$_4$(THF)$_2$ combine to form [(2,6-^{i}PrNCN)HfCl$_2$][Li(DME)$_3$] (**1**).[1] Obvious from the studies above, leaving the central aryl-CH proton in place prior to metalation results in bimetallic species with a bridging ligand. Part of the problem with the synthesis of **1** is salt separation during purification. A remedy is to alkylate and create a more soluble complex. Thus, generating **1** in situ and adding 2 equiv of MeLi provides colorless [(2,6-^{i}PrNCN)HfMe$_2$][Li(DME)$_2$] (**23**) in 35% yield (eq 12).

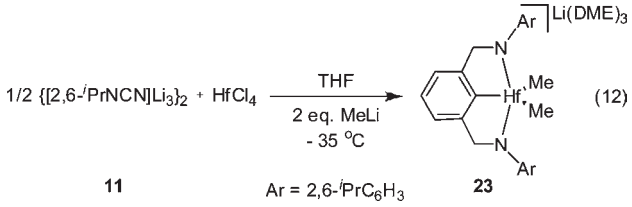

Exhibiting C_{2v}-symmetry in solution, the ^{1}H NMR (CDCl$_3$) spectrum of **23** reveals a singlet for the methyl protons at −0.49 ppm, and two doublets and one methine appear at 1.41, 1.39, and 4.26 ppm, respectively, for the ^{i}Pr groups. The furthest downfield signal in the ^{13}C{^{1}H} NMR (CDCl$_3$) spectrum of **23** is at 205.7 ppm and attributable to the C$_{ipso}$-Hf carbon. The corresponding C$_{ipso}$ in the dichloride complex **1** resonates slightly upfield at 201.5 ppm, and for [(3,5-MeNCN)$_2$Hf][Li$_2$(DME)$_2$] (**2**) it appears at 204.3 ppm.[1] Symmetric Hf-CH$_3$ carbons appear at 50.6 ppm, and the CH$_2$N carbon resonates at 72.5 ppm. Signals attributable to two equivalent DME molecules bound to Li$^+$ appear at 71.0 (CH$_3$OCH$_2$$CH_2OCH_3$)

(28) (a) Burger, H.; Wiegel, K.; Thewalt, U.; Schomburg, D. *J. Organomet. Chem.* **1975**, *87*, 301–309. (b) Brauer, D. J.; Burger, H.; Wiegel, K. *J. Organomet. Chem.* **1978**, *150*, 215–231. (c) Burger, H.; Beiersdorf, D. *Z. Anorg. Allg. Chem.* **1979**, *459*, 111–118. (d) Burger, H.; Geschwandtner, W.; Liewald, G. R. *J. Organomet. Chem.* **1983**, *259*, 145–156. (e) Herrmann, W. A.; Denk, M.; Albach, R. W.; Behm, J.; Herdtweck, E. *Chem. Ber.* **1991**, *124*, 683–689. (f) Guerin, F.; Mcconville, D. H.; Vittal, J. J. *Organometallics* **1995**, *14*, 3154–3156. (g) Scollard, J. D.; Mcconville, D. H.; Vittal, J. J. *Organometallics* **1995**, *14*, 5478–5480. (h) Guerin, F.; McConville, D. H.; Payne, N. C. *Organometallics* **1996**, *15*, 5085–5089. (i) Guerin, F.; McConville, D. H.; Vittal, J. J. *Organometallics* **1996**, *15*, 5586–5590. (j) Scollard, J. D.; McConville, D. H.; Vittal, J. J. *Organometallics* **1997**, *16*, 4415–4420.

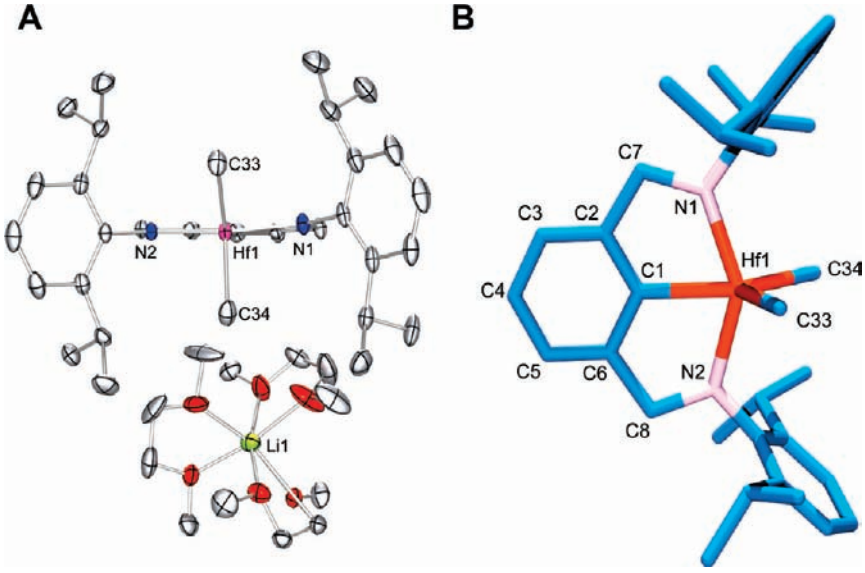

Figure 10. (**A**) Ortep drawing of the molecular structure of [2,6-^{i}PrNCNHfCl$_2$][Li(DME)$_3$] (**23**) with ellipsoids presented at the 50% probability level and hydrogen atoms removed for clarity. (**B**) Alternative perspective of **23** without the cation. Selected bond lengths (Å) and angles (deg): Hf1−N1, 2.1318(14); Hf1−N2, 2.1251(13); Hf1−C1, 2.2191(16); Hf1−C33, 2.2555(18); Hf1−C34, 2.2310(19); N1−Hf1−N2, 143.89(5); C1−Hf1−C33, 131.72(7); C1−Hf1−C34, 120.518(7); C33−Hf1−C34, 108.09(8).

and 59.6 ($CH_3OCH_2CH_2OCH_3$), which are shifted from free DME in $CDCl_3$ (71.8 and 59.08).

Complementary to the solution-state characterization, a single crystal X-ray diffraction experiment confirms the trianionic form of the ligand on **23** and its C_{2v} solid-state symmetry.[29] Figure 10 depicts two different perspectives of the molecular structure of **23**, Table 2 lists crystallographic refinement data, and a full list of bond lengths and angles appears in the Supporting Information. The geometry of the hafnium ion deviates from trigonal bipyramidal along the N−Hf−N axis. Instead of 180°, the five-atom metallocycle creates a N−Hf−N angle of 143.89(5)°.

In **23**, the Hf ion rests within the trigonal plane,[1,30] and the methyl groups create a 108.09(8)° angle between them, but are not symmetrically displaced. Hf1−C33 (2.2555(4) Å) is 0.0245(19) Å longer than Hf1−C34 (2.2310(19) Å), and an 11.54(9)° difference results between C1−Hf1−C33 (131.72(7)°) and C1−Hf1−C34 (120.18(7)°). No obvious electronic rationale explains this observation, and it must be due to the closer proximity of the Li(DME)$_3$ counterion complex to C34 in the lattice. The closest distances between C34−Li and C33−Li are approximately 4.9 and 6.0 Å, respectively.

Conclusions

Preparation of NCN ligand transmetalation reagents is straightforward. *N*,*N*′-[1,3-phenylenebis(methylene)]bis-2,6-diisopropylaniline [2,6-^{i}PrNCN]H$_3$ (**8**) was converted to the *N*,*N*′-substituted Si(IV), Sn(IV), Mg(II), and Zn(II) derivatives. Figure 11 depicts three different structural motifs that occur depending on the metal ion chosen for transmetalation.

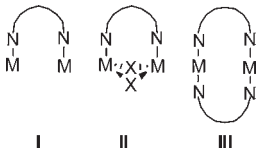

Figure 11. Structural motifs observed for diamido NCN transmetalation reagents.

The different arrangements are as follows: (I) one ligand binds two independent metal ions, (II) one ligand binds two metal ions bridged by mutual counterions, and (III) two ligands bind two independent metals ions. None of the precursors **9-Si**, **9-Sn**, **12**, **13**, or **17** undergo transmetalation to form a trianionic pincer complex. However, it is conceivable these reagents will find use as M-diamido precursors. For instance, {[2,6-^{i}PrNCHN]Li$_2$}$_2$ (**10**)[15a] reacts smoothly with ZrCl$_2$(NMe$_2$)$_2$(THF)$_2$ to form [2,6-^{i}PrNCHN]Zr(NMe$_2$)$_2$ **21**, but the ligand functions as a diamide with an intact aromatic C−H bond. Two new NCN derivatives were prepared with the intention of probing metalation reactions with both a more rigid and more flexible framework than **8**. As such, the flexible extended arm [3,5-CF$_3$N^{C}C^{C}N]H$_3$ (**16**) and the rigid anthracene [3,5-CF$_3$N^{C}C$_{anth}$^{C}N]H$_3$ (**18**) precursors were prepared and characterized. Metalation with M(NMe$_2$)$_4$ (M = Hf, and Zr) results in the bimetallic complexes {(μ-3,5-CF$_3$N^{C}CH^{C}N)Zr(NMe$_2$)$_3$NHMe$_2$}$_2$ (**19**) and (μ-3,5-CF$_3$N^{C}CH$_{anth}$^{C}N){Hf(NMe$_2$)$_3$NHMe$_2$}$_2$ (**20**). The more flexible ligand adopts the structural motif **III** (Figure 11), and the "rigid" anthracene version only allows one ligand to bind two metal ions, akin to type **I** (Figure 11). From this study it appears that metalation without prior activation of the central aromatic C−H bond predisposes the formation of bimetallics. In addition, ligand precursors possessing a flexible CH$_2$ group in the pincer arm are more prone to bimetallic species, considering the OCO derivatives (**B**; Figure 1) readily chelate to form trianionic pincer complexes.[2,3b,5,6,8] Removing the backbone C−H bond prior to metalation can provide trianionic pincer complexes, but

(29) As a single crystal the Li ion is coordinated by three DME solvent molecules, but routine isolation of **23** provides a composition with only two DME.

(30) [(2,6-^{i}PrNCN)HfCl$_2$][Li(DME)$_3$] (**1**) is distorted square pyramidal, and the Hf ion sits 0.4 Å above the basal plane.

access to trilithio or other trialkali salts of a variety of NCN derivatives is not likely. An attempt to form a trilithio salt of **16** results in lithiation of the CH_2 group and additional aromatic sites. Ultimately the trianionic pincer complex [2,6-^{i}PrNCNHfMe$_2$][Li(DME)$_2$] (**23**) forms when {[2,6-^{i}PrNCN]Li$_3$}$_2$ (**11**) reacts with $HfCl_4(THF)_2$ in THF followed by alkylation with MeLi. By alkylating, the yield and scale improves over the previous synthesis of the dichloride complex [(2,6-^{i}PrNCN)HfCl$_2$][Li(DME)$_3$] (**1**) because **23** is insoluble in Et_2O.[1] Complex **23** precipitates cleanly from DME upon slow addition of Et_2O, whereas **1** remains dissolved, complicating isolation. We continue to search for conditions that yield trianionic pincer complexes and are concentrating our efforts by starting with the parent neutral ligands and M-alkyl substrates to eliminate alkanes as the thermodynamic impetus.

Acknowledgment. A.S.V. thanks UF, the ACS−PRF-(G) (#44063-G3), NSF CAREER (CHE-0748408), and the Camille and Henry Dreyfus Foundation for financial support. K.P.M. and A.R.C. are UF Alumni Fellows. K. A.A. thanks the NSF (CHE-0821346) and UF for funding the purchase of X−ray equipment.

Supporting Information Available: Text describing experimental procedures, analytical, spectroscopic, crystallographic data, tables of bond lengths and angles, and cif files. This material is available free of charge via the Internet at http://pubs.acs.org.